

# Traffic Flow Theory

Sven Maerivoet\* and Bart De Moor  
Department of Electrical Engineering ESAT-SCD (SISTA)<sup>†</sup>,  
Katholieke Universiteit Leuven  
Kasteelpark Arenberg 10, 3001 Leuven, Belgium

(Dated: February 2, 2008)

The scientific field of traffic engineering encompasses a rich set of mathematical techniques, as well as researchers with entirely different backgrounds. This paper provides an overview of what is currently the state-of-the-art with respect to traffic flow theory. Starting with a brief history, we introduce the microscopic and macroscopic characteristics of vehicular traffic flows. Moving on, we review some performance indicators that allow us to assess the quality of traffic operations. A final part of this paper discusses some of the relations between traffic flow characteristics, i.e., the fundamental diagrams, and sheds some light on the different points of view adopted by the traffic engineering community.

PACS numbers: 02.50.-r,45.70.Vn,89.40.-a

Keywords: xxx

## Contents

<b>I. A brief history of traffic flow theory</b>	2	4. A note on the transitions between different regimes	17
<b>II. Microscopic traffic flow characteristics</b>	3	B. Correlations between traffic flow characteristics	17
A. Vehicle related variables	3	1. The historic origin of the fundamental diagram	17
B. Traffic flow characteristics	3	2. The general shape of a fundamental diagram	18
<b>III. Macroscopic traffic flow characteristics</b>	4	3. Empirical measurements	21
A. Density	5	C. Capacity drop and the hysteresis phenomenon	22
1. Mathematical formulation	5	D. Kerner's three-phase theory	23
2. Passenger car units	6	1. Free flow, synchronised flow, and wide-moving jam	23
B. Flow	6	2. Fundamental hypothesis of three-phase traffic theory	24
1. Mathematical formulation	6	3. Transitions towards a wide-moving jam	24
2. Oblique cumulative plots	7	4. From descriptions to simulations	25
C. Occupancy	8	E. Theories of traffic breakdown	25
D. Mean speed	9	<b>VI. Conclusions</b>	27
1. Mathematical formulation	9	<b>A. Glossary of terms</b>	27
2. Fundamental relation of traffic flow theory	10	1. Acronyms and abbreviations	27
E. Moving observer method and floating car data	11	2. List of symbols	28
<b>IV. Performance indicators</b>	12	<b>Acknowledgements</b>	30
A. Peak hour factor	12	<b>References</b>	30
B. Travel times and their reliability	12	The scientific field of traffic engineering encompasses a rich set of mathematical techniques, as well as researchers with entirely different backgrounds. This paper provides an overview of what is currently the state-of-the-art with respect to traffic flow theory. Starting with a brief history, we introduce the microscopic and macroscopic characteristics of vehicular traffic flows. Moving on, we review some performance indicators that allow us to assess the quality of traffic operations. A final part of this paper discusses some of the relations between traffic flow characteristics, i.e., the fundamental diagrams, and sheds some light on the different points of view adopted by the traffic engineering community.	
1. Travel time definitions	12	Because of the large diversity of the scientific field (en-	
2. Queueing delays	13		
3. An example of travel time estimation using cumulative plots	13		
4. Reliability and robustness properties	14		
C. Level of service	14		
D. Efficiency	15		
<b>V. Fundamental diagrams</b>	16		
A. Traffic flow regimes	16		
1. Free-flow traffic	16		
2. Capacity-flow traffic	16		
3. Congested, stop-and-go, and jammed traffic	16		

<sup>†</sup>Phone: +32 (0) 16 32 17 09 Fax: +32 (0) 16 32 19 70

URL: <http://www.esat.kuleuven.be/scd>

\*Electronic address: [sven.maerivoet@esat.kuleuven.be](mailto:sven.maerivoet@esat.kuleuven.be)

gineers, physicists, mathematicians, . . . all lack a unified standard or convention), one of the principal aims of this paper is to define both a *logical and consistent terminology and notation*. It is our strong belief that such a consistent notation is a necessity when it comes to creating order in the ‘zoo of notations’ that in our opinion currently exists. For a concise but complete overview of all abbreviations and notations proposed and adopted throughout this paper, we refer the reader to appendix A.

## I. A BRIEF HISTORY OF TRAFFIC FLOW THEORY

Historically, traffic engineering got its roots as a rather practical discipline, entailing most of the time a common sense of its practitioners to solve particular traffic problems. However, all this changed at the dawn of the 1950s, when the scientific field began to mature, attracting engineers from all sorts of trades. Most notably, John Glen Wardrop instigated the evolving discipline now known as traffic flow theory, by describing traffic flows using mathematical and statistical ideas [115].

During this highly active period, mathematics established itself as a solid basis for theoretical analyses, a phenomenon that was entirely new to the previous, more ‘rule-of-thumb’ oriented, line of reasoning. Two examples of the progress during this decade, include the fluid-dynamic model of Michael James Lighthill, Gerald Beresford Whitham, and Paul Richards (or the *LWR model* for short) for describing traffic flows [72, 102], and the car-following experiments and theories of the club of people working at General Motors’ research laboratory [17, 40, 41, 50]. Simultaneous progress was also made on the front of economic theory applied to transportation, most notably by the publication of the ‘BMW trio’, Martin J. Beckmann, Charles Bartlett McGuire, and Christopher B. Winsten [6].

From the 1960s on, the field evolved even further with the advent of the early personal computers (although at that time, they could only be considered as mere computing units). More control-oriented methods were pursued by engineers, as a means for alleviating congestion at tunnels and intersections, by e.g., adaptively steering traffic signal timings. Nowadays, the field has been kindly embraced by the industry, resulting in what is called *intelligent transportation systems* (ITS), covering nearly all aspects of the transportation community.

In spite of the intense booming during the 1950s and 1960s, all progress seemingly came to sudden stop, as there were almost no significant results for the next two decades (although there are some exceptions, such as the significant work of Ilya Prigogine and Robert Herman’s, who developed a traffic flow model based on a gas-kinetic analogy [101]). One of the main reasons for this, stems from the fact that many of the involved key players returned to their original scientific disciplines, after exhausting the application of their techniques to the transportation problem [99]. Note that despite this calm period, the application of control theory to transporta-

tion started finding new ways to alleviate local congestion problems.

At the beginning of the 1990s, researchers found a revived interest in the field of traffic flow modelling. On the one hand, researchers’ interests got kindled again by the appealing simplicity of the LWR model, whereas on the other hand one of the main boosts came from the world of statistical physics. In this latter framework, physicists tried to model many particle systems using simple and elegant behavioural rules. As an example, the now famous particle hopping (cellular automata) model of Kai Nagel and Michael Schreckenberg [92] still forms a widely-cited basis for current research papers on the subject.

In parallel with this kind of modelling approach, many of the old ‘beliefs’ (e.g., the fluid-dynamic approach to traffic flow modelling) started to get questioned. As a consequence, a plethora of models quickly found its way to the transportation community, whereby most of these models didn’t give a thought as to whether or not their associated phenomena corresponded to real-life traffic observations.

We note here that, whatever the modelling approach may be, researchers should always compare their results to the reality of the physical world. Ignoring this basic step, reduces the research in our opinion to nothing more than a mathematical exercise !

As the international research community began to spawn its traffic flow theories, Robert Herman aspired to bring them all together in december 1959. This led to the tri-annual organisation of the *International Symposium on Transportation and Traffic Theory* (ISTTT), by some heralded as ‘the Olympics of traffic theory’ because the symposium talks about the fundamentals underlying transportation and traffic phenomena. Another example of the evolution of recent developments with respect to the parallels between traffic flows and granular media, is the bi-annual organisation of the workshop on *Traffic and Granular Flow* (TGF), a platform for exchanging ideas by bringing together researchers from various scientific fields.

Nowadays, the research and application of traffic flow theory and intelligent transportation systems continues. The scientific field has been largely diversified, encompassing a broad range of aspects related to sociology, psychology, the environment, the economy, . . . The global avidity of the field can be witnessed by the exponentially growing publication output. Keeping our previous comment in mind, researchers from time to time just seem to ‘add to the noise’ (mainly due to the sheer diversity of the literature body), although there occasionally exist exceptions such as the late Newell, as subtly pointed out by Michael Cassidy in [100].

As a final word, we refer the reader to two personalised views on the history of traffic flow theory, namely the musings of the late Gordon Newell and Denos Gazis [42, 99]. We furthermore invite the reader to cast a glance at the ending pages of Wardrop’s paper [115], in which a rather colourful discussion on the introduction of mathematics to traffic flow theory has been written down.

## II. MICROSCOPIC TRAFFIC FLOW CHARACTERISTICS

Road traffic flows are composed of drivers associated with individual vehicles, each of them having their own characteristics. These characteristics are called *microscopic* when a traffic flow is considered as being composed of such a stream of vehicles. The dynamical aspects of these traffic flows are formed by the underlying interactions between the drivers of the vehicles. This is largely determined by the behaviour of each driver, as well as the physical characteristics of the vehicles.

Because the process of participating in a traffic flow is heavily based on the behavioural aspects associated with human drivers [39], it would seem important to include these human factors into the modelling equations. However, this leads to a severe increase in complexity, which is not always a desired artifact [76]. However, in the remainder of this section, we always consider a vehicle-driver combination as a single entity, taking only into account some vehicle related traffic flow characteristics.

Note that despite our previous remarks, we do not debate the necessity of a psychological treatment of traffic flow theory. As the research into driver behaviour is gaining momentum, a lot of attention is gained by promising studies aimed towards driver and pedestrian safety, average reaction times, the influence of stress levels, aural and visual perceptions, ageing, medical conditions, fatigue, ...

### A. Vehicle related variables

Considering individual vehicles, we can say that each vehicle  $i$  in a lane of a traffic stream has the following informational variables:

- a *length*, denoted by  $l_i$ ,
- a *longitudinal position*, denoted by  $x_i$ ,
- a *speed*, denoted by  $v_i = \frac{dx_i}{dt}$ ,
- and an *acceleration*, denoted by  $a_i = \frac{dv_i}{dt} = \frac{d^2x_i}{dt^2}$ .

Note that the position  $x_i$  of a vehicle is typically taken to be the position of its rear bumper. In this first approach, a vehicle's other spatial characteristics (i.e., its width, height, and lane number) are neglected. And in spite of our narrow focus on the vehicle itself, the above list of variables is also complemented with a driver's *reaction time*, denoted by  $\tau_i$ .

With respect to the acceleration characteristics, it should be noted that these are in fact not only dependent on the vehicle's engine, but also on e.g., the road's inclination, being a non-negligible factor that plays an important role

in the forming of congestion at bridges and tunnels. We do not use the derivative of the acceleration, called *jerk*, *jolt*, or *surge* (jerk is also used to represent the smoothness of the *acceleration noise* [82]).

Except in the acceleration capabilities of a vehicle, we ignore the physical forces that act on a vehicle, e.g., the earth's gravitational pull, road and wind friction, centrifugal forces, ... A more elaborate explanation of these forces can be found in [27].

### B. Traffic flow characteristics

Referring to Fig. 1, we can consider two consecutive vehicles in the same lane in a traffic stream: a follower  $i$  and its leader  $i + 1$ . From the figure, it can be seen that vehicle  $i$  has a certain *space headway*  $h_{s_i}$  to its predecessor (it is expressed in metres), composed of the distance (called the *space gap*)  $g_{s_i}$  to this leader and its own *length*  $l_i$ :

$$h_{s_i} = g_{s_i} + l_i. \quad (1)$$

By taking, as stated before, the rear bumper as a vehicle's position, the space headway  $h_{s_i} = x_{i+1} - x_i$ . The space gap is thus measured from a vehicle's front bumper to its leader's rear bumper.

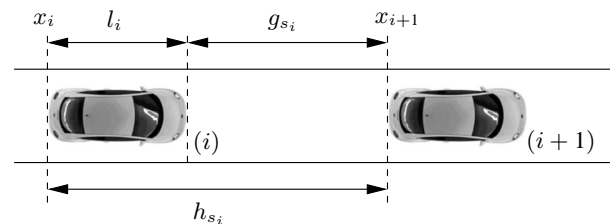


FIG. 1: Two consecutive vehicles (a follower  $i$  at position  $x_i$  and a leader  $i + 1$  at position  $x_{i+1}$ ) in the same lane in a traffic stream. The follower has a certain space headway  $h_{s_i}$  to its leader, equal to the sum of the vehicle's space gap  $g_{s_i}$  and its length  $l_i$ .

Analogously to equation (1), each vehicle also has a *time headway*  $h_{t_i}$  (expressed in seconds), consisting of a *time gap*  $g_{t_i}$  and an *occupancy time*  $\rho_i$ :

$$h_{t_i} = g_{t_i} + \rho_i. \quad (2)$$

Both space and time headways can be visualised in a *time-space diagram*, such as the one in Fig. 2. Here, we have shown the two vehicles  $i$  and  $i + 1$  as they are driving. Their positions  $x_i$  and  $x_{i+1}$  can be plotted with respect to time, tracing out two *vehicle trajectories*. As the time direction is horizontal and the space direction is vertical, the vehicles' respective speeds can be derived by taking the tangents of the trajectories (for simplicity, we have assumed that both vehicles travel at the same constant speed, resulting in parallel linear trajectories).

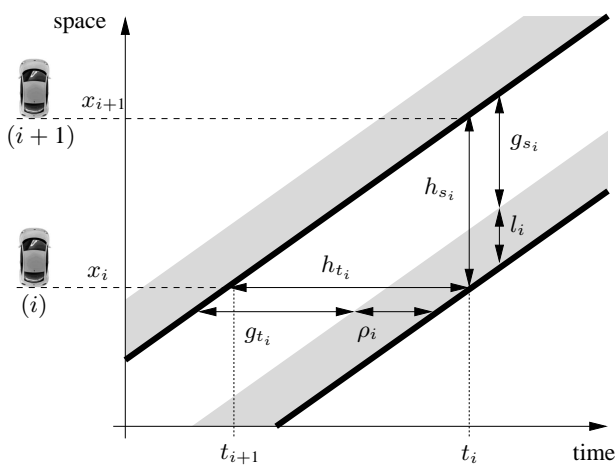


FIG. 2: A time-space diagram showing two vehicle trajectories  $i$  and  $i + 1$ , as well as the space and time headway  $h_{s_i}$  and  $h_{t_i}$  of vehicle  $i$ . Both headways are composed of the space gap  $g_{s_i}$  and the vehicle length  $l_i$ , and the time gap  $g_{t_i}$  and the occupancy time  $\rho_i$ , respectively. The time headway can be seen as the difference in time instants between the passing of both vehicles, respectively at  $t_{i+1}$  and  $t_i$  (diagram based on [74]).

Accelerating vehicles have steep inclining trajectories, whereas those of stopped vehicles are horizontal.

When the vehicle's speed is constant, the time gap is the amount of time necessary to reach the current position of the leader when travelling at the current speed (i.e., it is the elapsed time an observer at a fixed location would measure between the passing of two consecutive vehicles). Similarly, the occupancy time can be interpreted as the time needed to traverse a distance equal to the vehicle's own length at the current speed, i.e.,  $\rho_i = l_i/v_i$ ; this corresponds to the time the vehicle needs to pass the observer's location. Both equations (1) and (2) are furthermore linked to the vehicle's speed  $v_i$  as follows [27]:

$$\frac{h_{s_i}}{h_{t_i}} = \frac{g_{s_i}}{g_{t_i}} = \frac{l_i}{\rho_i} = v_i. \quad (3)$$

As the above definitions deal with what is called single-lane traffic, we can easily extend them to multi-lane traffic. In this case, four extra space gaps — related to the vehicles in the neighbouring lanes — are introduced, namely  $g_{s_i}^{l,f}$  at the left-front,  $g_{s_i}^{l,b}$  at the left-back,  $g_{s_i}^{r,f}$  at the right-front, and  $g_{s_i}^{r,b}$  at the right-back. The four corresponding space headways,  $h_{s_i}^{l,f}$ ,  $h_{s_i}^{l,b}$ ,  $h_{s_i}^{r,f}$ , and  $h_{s_i}^{r,b}$ , are introduced in a similar fashion. The extra time gaps and headways are derived in complete analogy, leading to the four time gaps  $g_{t_i}^{l,f}$ ,  $g_{t_i}^{l,b}$ ,  $g_{t_i}^{r,f}$ , and  $g_{t_i}^{r,b}$ , and the four corresponding time headways  $h_{t_i}^{l,f}$ ,  $h_{t_i}^{l,b}$ ,  $h_{t_i}^{r,f}$ , and  $h_{t_i}^{r,b}$ .

In single-lane traffic, vehicles always keep their relative order, a principle sometimes called *first-in, first-out* (FIFO) [24]. For multi-lane traffic however, this principle is no longer obeyed due to overtaking manoeuvres, resulting in vehicle trajectories that cross each other. If the same time-space diagram were to be drawn for only one lane (in multi-lane traffic), then some vehicles'

trajectories would suddenly appear or vanish at the point where a lane change occurred.

In some traffic flow literature, other nomenclature is used: *space* for the space headway, *distance* or *clearance* for the space gap, and *headway* for the time headway. Because this terminology is confusing, we propose to use the unambiguously defined terms as described in this section.

### III. MACROSCOPIC TRAFFIC FLOW CHARACTERISTICS

When considering many vehicles simultaneously, the time-space diagram mentioned in section II B can be used to faithfully represent all traffic. In Fig. 3 we show the evolution of the system, as we have traced the trajectories of all the individual vehicles' movements. This time-space diagram therefore provides a complete picture of all traffic operations that are taking place (accelerations, decelerations, ...).

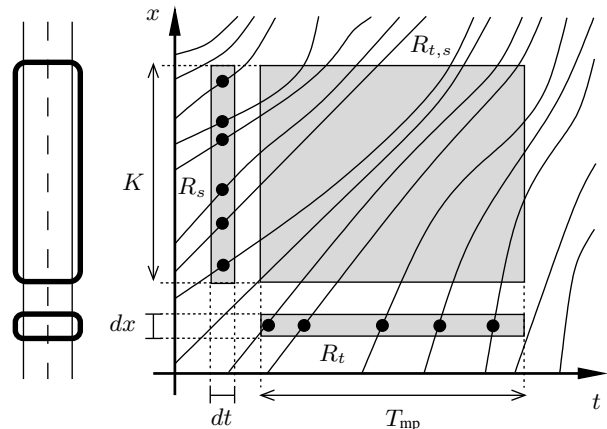


FIG. 3: A time-space diagram showing several vehicle trajectories and three measurement regions  $R_t$ ,  $R_s$ , and  $R_{t,s}$ . These rectangular regions are bounded in time and space by a measurement period  $T_{mp}$  and a road section of length  $K$ . The black dots represent the individual measurements.

Instead of considering each vehicle in a traffic stream individually, we now 'zoom out' to a more aggregate *macroscopic* level (traffic streams are regarded e.g., as a fluid). In the remainder of this section, we will measure some macroscopic traffic flow characteristics based on the shown time-space diagram. To this end, we define three measurement regions:

- $R_t$  corresponding to measurements at a single fixed location in space ( $dx$ ), during a certain time period  $T_{mp}$ . An example of this is a single inductive loop detector (SLD) embedded in the road's concrete.
- $R_s$  corresponding to measurements at a single instant in time ( $dt$ ), over a certain road section of length  $K$ . An example of this is an aerial photograph.

- $R_{t,s}$  corresponding to a general measurement region. Although it can have any shape, in this case we restrict ourselves to a rectangular region in time and space. An example of this is a sequence of images made by a video camera detector.

With respect to the size of these measurement regions, some caution is advised: a too large measurement region can mask certain effects of traffic flows, possibly ignoring some of the dynamic properties, whereas a too small measurement region may obstruct a continuous treatment, as the discrete, microscopic nature of traffic flows becomes apparent.

Using these different methods of observation, we now discuss the measurement of four important macroscopic traffic flow characteristics: density, flow, occupancy, and mean speed. We furthermore give a short discussion on the moving observer method and the use of floating car data.

With respect to some naming conventions on roadways, two different ‘standards’ exist for some of the encountered terminology, namely the American and the British standard. Examples are: the classic multi-lane high-speed road with on- and off-ramps, which is called a *freeway* or a *super highway* (American), or an *arterial* or *motorway* (British). A main road with intersections is called an *urban highway* (American) or a *carriageway* (British). In this dissertation, we have chosen to adopt the British standard. Finally, in contrast to Great Britain and Australia, we assume that for low-density traffic, everybody drives on the right instead of the left lane.

## A. Density

The macroscopic characteristic called *density* allows us to get an idea of how crowded a certain section of a road is. It is typically expressed in number of vehicles per kilometre (or mile). Note that the concept of density totally ignores the effects of traffic composition and vehicle lengths, as it only considers the abstract quantity ‘number of vehicles’.

Because density can only be *measured* in a certain spatial region (e.g.,  $R_s$  in Fig. 3), it is *computed* for temporal regions such as region  $R_t$  in Fig. 3. When density can not be exactly measured or computed, or when density measurements are faulty, it has to be *estimated*. To this end, several available techniques exist e.g., based on explicit simulation using a traffic flow propagation model [90], based on a vehicle reidentification system [21], based on a complete traffic state estimator using an extended Kalman filter [114], or based on a non-linear adaptive observer [3], ...

## 1. Mathematical formulation

Using the spatial region  $R_s$ , the density  $k$  for single-lane traffic is defined as:

$$k = \frac{N}{K}, \quad (4)$$

with  $N$  the number of vehicles present on the road segment. If we consider multi-lane traffic, we have to sum the partial densities  $k_l$  of each of the  $L$  lanes as follows:

$$k = \sum_{l=1}^L k_l = \frac{1}{K} \sum_{l=1}^L N_l, \quad (5)$$

in which  $N_l$  now denotes the number of vehicles present in lane  $l$  (equation (5) is *not* the same as averaging over the partial densities of each lane)[122].

In general, density can be defined as *the total time spent by all the vehicles in the measurement region, divided by the area of this region* [27, 36]. This generalisation allows us to compute the density at a point using the measurement region  $R_t$ :

$$k = \frac{\sum_{i=1}^N T_i}{T_{mp} dx} = \frac{1}{T_{mp} dx} \sum_{i=1}^N \frac{dx}{v_i} = \frac{1}{T_{mp}} \sum_{i=1}^N \frac{1}{v_i}, \quad (6)$$

with  $T_i$  the travel time and  $v_i$  the speed of the  $i^{\text{th}}$  vehicle. Extending the previous derivation to multi-lane traffic is done straightforward using equation (5):

$$k = \frac{1}{T_{mp}} \sum_{l=1}^L \sum_{i=1}^{N_l} \frac{1}{v_{i,l}}, \quad (7)$$

with now  $v_{i,l}$  denoting the speed of the  $i^{\text{th}}$  vehicle in lane  $l$ .

As we now can obtain the density in both spatial and temporal regions,  $R_s$  and  $R_t$  respectively, it would seem a logical extension to find the density in the region  $R_{t,s}$ . In order to do this, however, we need to know the travel times  $T_i$  of the individual vehicles, as can be seen in equation (6). Because this information is not always available, and in most cases rather difficult to measure, we use a different approach, corresponding to the temporal average of the density. Assuming that at each time step  $t$ , during a certain time period  $T_{mp}$ , the density  $k(t)$  is known in consecutive regions  $R_s$ , the generalised definition leads to the following formulation:

$$k = \begin{cases} \frac{1}{T_{mp}} \int_{t=0}^{T_{mp}} k(t) dt & \text{(continuous),} \\ \frac{1}{T_{mp}} \sum_{t=1}^{T_{mp}} k(t) & \text{(discrete).} \end{cases} \quad (8)$$

For multi-lane traffic, combining equations (5) and (8) results in the following formula for computing the density in region  $R_{t,s}$  using measurements in discrete time:

$$k = \frac{1}{T_{\text{mp}} K} \sum_{t=1}^{T_{\text{mp}}} \sum_{l=1}^L N_l(t), \quad (9)$$

where  $N_l(t)$  denotes the number of vehicles present in lane  $l$  at time  $t$ .

There exists a relation between the macroscopic traffic flow characteristics and those microscopic characteristics defined in section II B. For the density  $k$ , this relation is based on the average space headway  $\bar{h}_s$  [27, 115]:

$$k = \frac{N}{K} = \frac{N}{\sum_{i=1}^N h_{s_i}} = \frac{1}{\frac{1}{N} \sum_{i=1}^N h_{s_i}} = \frac{1}{\bar{h}_s}, \quad (10)$$

with  $\bar{h}_s^{-1}$  the reciprocal of the average space headway.

## 2. Passenger car units

When considering heterogeneous traffic flows (i.e., traffic streams composed of different types of vehicles), operating agencies usually don't express the macroscopic traffic flow characteristics using the raw number of vehicles, but rather employ the notion of *passenger car units* (PCU). These PCUs, sometimes also called *passenger car equivalents* (PCE), try to take into account the spatial differences between vehicle types. For example, by denoting one average passenger car as 1 PCU, a truck in the same traffic stream can be considered as 2 PCUs (or even higher and fractional values for trailer trucks).

Let us finally note that, because density is essentially defined as a spatial measurement, it is one of the most difficult quantities to obtain. It is interesting to notice that at this moment, it is theoretically possible for video cameras to measure density over a short spatial region. However, to our knowledge there currently exists no commercial implementation.

## B. Flow

Whereas density typically is a spatial measurement, *flow* can be considered as a temporal measurement (i.e., region  $R_t$ ). Flow, which we use as a shorthand for rate of flow, is typically expressed as an hourly rate, i.e., in number of vehicles per hour. Note that sometimes other synonyms such as *intensity*, *flux*, *throughput*, *current*, or *volume* [123] are used, typically depending on a person's scientific background (e.g., engineering, physics, ...).

## 1. Mathematical formulation

Measuring the flow  $q$  in region  $R_t$  for single-lane traffic, is done using the following equation, which is based on raw vehicle counts:

$$q = \frac{N}{T_{\text{mp}}}, \quad (11)$$

with  $N$  the number of vehicles that has passed the detector's site. For multi-lane traffic, we sum the partial flows of each of the  $L$  lanes:

$$q = \sum_{l=1}^L q_l = \frac{1}{T_{\text{mp}}} \sum_{l=1}^L N_l, \quad (12)$$

with now  $N_l$  denoting the number of vehicles that passed the detector's site in lane  $l$ . Note that we assume that each lane has its own detector, otherwise we would be dealing with an average flow across all the lanes.

Generally speaking, flow can be defined as *the total distance travelled by all the vehicles in the measurement region, divided by the area of this region* [27, 36]. In analogy with equation (6), this generalisation allows us to compute the flow using the spatial measurement region  $R_s$ :

$$q = \frac{\sum_{i=1}^N X_i}{K dt} = \frac{1}{K} \sum_{i=1}^N v_i dt = \frac{1}{K} \sum_{i=1}^N v_i, \quad (13)$$

with now  $X_i$  the distance travelled by the  $i^{\text{th}}$  vehicle during the infinitesimal time interval  $dt$ . The extension to multi-lane traffic is straightforward:

$$q = \frac{1}{K} \sum_{l=1}^L \sum_{i=1}^{N_l} v_{i,l}. \quad (14)$$

Considering consecutive flow measurements in region  $R_{t,s}$ , we can derive a formulation corresponding to the temporal average of the flow, similar to that of equation (8). Assuming that at each time step  $t$ , during a certain time period  $T_{\text{mp}}$ , the flow  $q(t)$  is known in consecutive regions  $R_s$ , the generalised definition leads to the following equations:

$$q = \begin{cases} \frac{1}{T_{\text{mp}}} \int_{t=0}^{T_{\text{mp}}} q(t) dt & \text{(continuous),} \\ \frac{1}{T_{\text{mp}}} \sum_{t=1}^{T_{\text{mp}}} q(t) & \text{(discrete),} \end{cases} \quad (15)$$

For multi-lane traffic, combining equations (14) and (15) results in the following formula for computing the flow in region  $R_{t,s}$  using measurements in discrete time:

$$q = \frac{1}{T_{\text{mp}} K} \sum_{t=1}^{T_{\text{mp}}} \sum_{l=1}^L \sum_{i=1}^{N_l(t)} v_{i,l}(t), \quad (16)$$

where  $v_{i,l}(t)$  denotes the speed of the  $i^{\text{th}}$  vehicle in lane  $l$  at time  $t$ .

In analogy with equation (10), there exists a relation between the flow  $q$ , and the average time headway  $\bar{h}_t$  [27, 115]:

$$q = \frac{N}{T_{\text{mp}}} = \frac{N}{\sum_{i=1}^N h_{t_i}} = \frac{1}{\frac{1}{N} \sum_{i=1}^N h_{t_i}} = \frac{1}{\bar{h}_t}, \quad (17)$$

with  $\bar{h}_t^{-1}$  the reciprocal of the average time headway.

## 2. Oblique cumulative plots

As stated before, flows are always expressed as a rate. In contrast to this, we can also consider the raw vehicle counts at a certain location (i.e., measurement region  $R_t$ ). If we plot the cumulative number of passing vehicles (denoted by  $N$ ) with respect to time for different regions (e.g., inductive loop detectors), we get a set of curves such as the one in the left part of Fig. 4. These curves are called *cumulative plots* (or  $(t, N)$  diagrams), and although their origins date back as far as 1954 with the work of Karl Moskowitz [83], it was Gordon Newell who applied them later on to their full potential (initially in the context of queueing theory) [95, 96, 97, 98] (a similar method was applied by John Luke, in the field of continuum mechanics [25, 75]).

The key benefit of these cumulative plots, comes when comparing observations stemming from multiple detector stations at a closed section of the road that conserves the number of vehicles (i.e., no on- or off-ramps), in which case we also speak of *input-output diagrams*. If there are two detector stations, then the upstream and downstream stations measure the *input*, respectively *output*, of the section. Similarly like in queueing theory, the upstream curve is sometimes called the *arrival function*, whereas the downstream one is called the *departure function* [95]. As the method is based on counting the number of individual vehicles at each observation location (whereby each vehicle is numbered with respect to a single reference vehicle), this results in a monotonically increasing function  $N(t)$  (sometimes called the *Moskowitz function*, after its ‘inventor’), which increases each time a vehicles passes by. At each time instant  $t$ , the cumulative count is

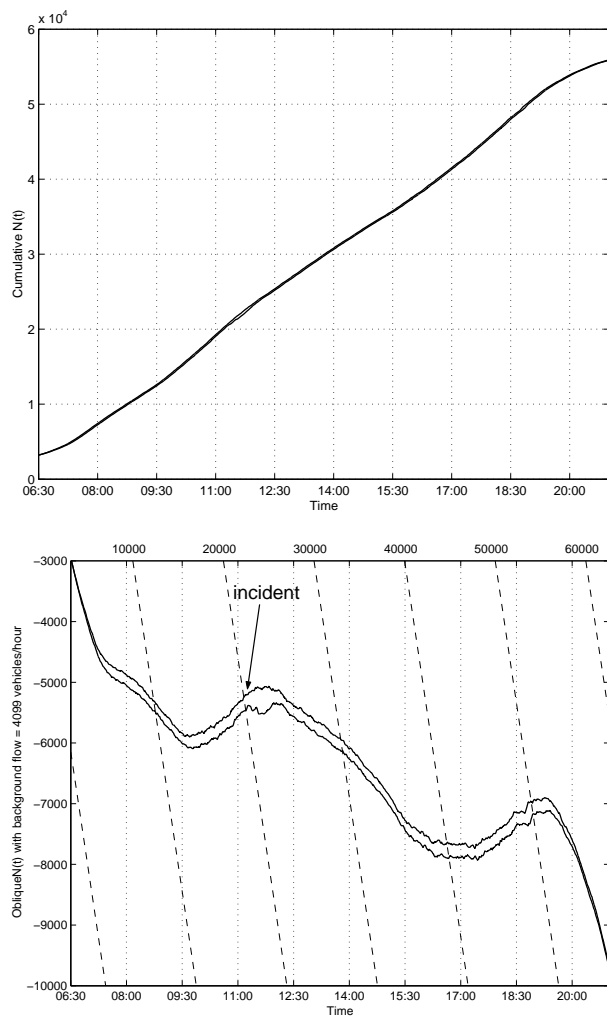


FIG. 4: *Left*: a standard cumulative plot showing the number of passing vehicles at two detector locations; due to the graph’s scale, both curves appear to lie on top of each other. *Right*: the same data but displayed using an oblique coordinate system, thereby enhancing the visibility (the dashed slanted lines have a slope corresponding to the subtracted background flow  $q_b \approx 4100$  vehicles per hour). We can see a queue (probably caused due to an incident) growing at approximately 11:00, dissipating some time later at approximately 12:30. The shown detector data was taken from single inductive loop detectors [113], covering all three lanes of the E40 motorway between Erpe-Mere and Wetteren, Belgium. The shown data was recorded at Monday April 4th, 2003 (the detectors’ sampling interval was one minute, the distance between the upstream and downstream detector stations was 8.1 kilometres).

defined as:

$$N(t) = \sum_{t'=t_0}^t q(t') = N(t-1) + q(t). \quad (18)$$

The time needed to travel from one location to another can easily be measured as the horizontal distance between the respective cumulative curves. Similarly, the vertical distance between these curves allows us to derive the accumulation of vehicles on the road section, which

gives an excellent indication of growing and dissipating queues (i.e., congestion). Furthermore, if we compute the slope of this function at each time instant  $t$ , we obtain the flow  $q(t) = [N(t + \Delta t) - N(t)]/\Delta t$ . Finally, because  $N(t)$  essentially is a step function, we can define a smooth approximation  $\tilde{N}(t)$ . This results in an everywhere differentiable function, allowing us to compute instantaneous flows and local densities as  $q = \partial\tilde{N}(t, x)/\partial t$  and  $k = -\partial\tilde{N}(t, x)/\partial x$ , respectively [27].

The main disadvantage of the method is the fact that these cumulative functions increase very rapidly, thereby masking the subtle differences between different curves. Cassidy and Windover therefore proposed to subtract a background flow  $q_b$  from these curves, resulting in functions  $N(t) - t q_b$  [13]. Based on this; Muñoz and Daganzo furthermore introduced enhanced clarity by overlaying this cumulative plot with a set of oblique lines with slope  $-q_b$  [88]. Choosing an appropriate value for  $q_b$ , allows us to nicely enhance the characteristic undulations that are expressed by the different oblique curves.

Note that before using these oblique plots, the cumulative plots from different detector stations need to be *synchronised*. To understand this, suppose a reference vehicle passes an upstream detector station at a certain time instant  $t_{\text{up}}$ ; after a certain time period, the vehicle reaches the downstream detector station at a later time instant  $t_{\text{down}}$ . The amount  $t_{\text{down}} - t_{\text{up}}$  is the time it takes to cross the distance between both detector stations, allowing the synchronisation mechanism to shift the respective cumulative curves over this time period (i.e., initialising them with the passing of the reference vehicle).

One way to achieve this, is by looking at the respective shapes of both cumulative curves during light traffic conditions (e.g., the early morning period when free-flow conditions are prevailing). The idea now is to shift one curve such that the difference between the two curves' shapes is minimal [86, 89, 118]. Note that other corrections may be necessary, as both detector stations can count a different number of vehicles (i.e., a systematic bias).

An example of an oblique plot can be seen in the right part of Fig. 4: the cumulative count at each time instant can be read from an axis that is perpendicular to the oblique (slanted) overlaid dashed lines (e.g., we can see a count of some 30000 vehicles at 14:00). Note that the accumulation can still be measured by the vertical distance between two curves (i.e., at a specific time instant), but the travel time should now be measured along one of the overlaid oblique lines. Such a pair of cumulative curves can be thought of as a flexible plastic garden hose: whenever there is an obstruction on the road, the outflow of the section will be blocked, resulting in a local thickening of this 'hose' (i.e., the accumulation of vehicles on the section).

Using these oblique cumulative plots, we can now inspect the traffic dynamics in much more detail than was previ-

ously possible. For example, looking again at the right part of Fig. 4, we can see how the specific traffic stream characteristics propagate from one detector station to another. Even more visible, is a queue that starts to grow at approximately 11:00 (i.e., the time of the appearance of a 'bulge'), dissipating at approximately 12:30. As data curves from upstream detectors lie above data curves from downstream detectors, we see a decrease in the road section's output. Careful investigation of the traffic data revealed that the detector stations recorded a rather low flow (approximately 2500 vehicles per hour as opposed to a nominal flow of 4500 vehicles per hour), whereby all vehicles drove at a low speed (between 20 and 60 km/h as opposed to 110 km/h). This gives sufficient evidence to conclude that an incident probably occurred shortly after 11:00, consequently obstructing a part of the road and leading to a build up of vehicles in the section.

Let us finally note that although oblique cumulative plots currently are not a mainstream technique used by the traffic community, we predict their rising popularity: they are one of the most simple, yet powerful, techniques for studying local traffic phenomena, giving traffic engineers practical insight into the formation of bottlenecks. Some recent examples include the work of Muñoz and Daganzo [85, 86, 87, 89], Cassidy and Bertini [7, 15], Cassidy and Mauch [16], and Bertini et al. [8].

### C. Occupancy

Notwithstanding the importance of measuring traffic density, most of the existing detector stations on the road are only capable of temporal measurements (i.e., region  $R_t$ ). If individual vehicle speeds can be measured, by double inductive loop detectors (DLD) for example, then density should be computed using equation (6).

However, in many cases these vehicle speeds are not readily available, e.g., when using single inductive loop detectors. The detector's logic therefore resorts to a temporal measurement called the *occupancy*  $\rho$ , which corresponds to the fraction of time the measurement location was occupied by a vehicle:

$$\rho = \frac{1}{T_{\text{mp}}} \sum_{i=1}^N o_{t_i}. \quad (19)$$

In the previous equation,  $o_{t_i}$  denotes the  $i^{\text{th}}$  vehicle's *on-time*, i.e., the time period during which it is present above the detector (it corresponds to the shaded area swept by a vehicle at a certain location  $x_i$  in Fig. 2). Note that this on-time actually corresponds to the effective vehicle length as seen by the detector, divided by the vehicle's speed [20]:

$$o_{t_i} = \frac{l_i + K_{\text{ld}}}{v_i}, \quad (20)$$



with  $l_i$  the vehicle's true length and  $K_{ld} > dx$  the finite, non-infinitesimal length of the detection zone. If we define  $\bar{o}_t$  as the average on-time (based on the vehicles that have passed the detector during the observation period), then we can establish a relation between the occupancy and the flow [27] using equations (11) and (19):

$$\rho = \left( \frac{N}{T_{mp}} \right) \left( \frac{1}{N} \sum_{i=1}^N o_{t_i} \right) = q \bar{o}_t. \quad (21)$$

Furthermore, it is as before possible to define the occupancy for generalised measurement regions, using the total space consumed by the shaded areas of vehicles in a time-space diagram (e.g., Fig. 2), divided by the area of the measurement region [14, 27, 36]. Continuing our discussion, assume that individual vehicle lengths and speeds are uncorrelated; it can then be shown that [20, 27]:

$$\rho = \bar{l} k \implies k = \frac{\rho}{\bar{l}}, \quad (22)$$

with  $\bar{l}$  the average vehicle length (note that this can correspond to the concept of passenger car units defined in section III A). Multiplying equation (22) by 100, allows us to express the occupancy as a percentage. For multi-lane traffic, the occupancy is derived in analogy to equation (7):

$$\rho = \sum_{l=1}^L \rho_l = \frac{1}{T_{mp}} \sum_{l=1}^L \sum_{i=1}^{N_l} o_{t_{i,l}}, \quad (23)$$

with now  $o_{t_{i,l}}$  the on-time of the  $i^{\text{th}}$  vehicle in lane  $l$ . Note that the total occupancy derived in this way, can exceed 1 (but is bounded by  $L$ ); if desired, it can be normalised through a division by  $L$  to obtain the *average occupancy*.

Note that if we apply equation (22) to measurement region  $R_s$  based on the density in equation (4), then the occupancy  $\rho$  can be written as:

$$\rho = \left( \frac{1}{\mathcal{N}} \sum_{i=1}^N l_i \right) \frac{\mathcal{N}}{K} = \frac{1}{K} \sum_{i=1}^N l_i. \quad (24)$$

So the occupancy now represents the 'real density' of the road, i.e., the physical space that all vehicles occupy.

In the past, density was sometimes referred to as *concentration*. Nowadays however, concentration is used in a more broad context, encompassing both density and occupancy whereby the former is meant to be a spatial measurement, as opposed to the latter which is considered to be a temporal measurement [39].

The final macroscopic characteristic to be considered, is the *mean speed* of a traffic stream; it is expressed in kilometres (or miles) per hour (the inverse of a vehicle's speed is called its *pace*). Note that speed is not to be confused with *velocity*; the latter is actually a vector, implying a direction, whereas the former could be regarded as the norm of this vector.

### 1. Mathematical formulation

If we base our approach on direct measurements of the individual vehicles' speeds, we can generally obtain the mean speed as *the total distance travelled by all the vehicles in the measurement region, divided by the total time spent in this region* [27, 36]. This gives the following derivations for the spatial and temporal regions,  $R_s$  and  $R_t$  respectively:

$$\bar{v}_s = \frac{\sum_{i=1}^N X_i}{\sum_{i=1}^N T_i} = \begin{cases} \frac{\sum_{i=1}^N v_i \mathcal{A}}{N \mathcal{A}} = \frac{1}{N} \sum_{i=1}^N v_i & (\text{region } R_s), \\ \frac{N \mathcal{A}}{\sum_{i=1}^N \frac{\mathcal{A}}{v_i}} = \frac{1}{\frac{1}{N} \sum_{i=1}^N \frac{1}{v_i}} & (\text{region } R_t), \end{cases} \quad (25)$$

with now  $X_i$  and  $T_i$  the distance, respectively time, travelled by the  $i^{\text{th}}$  vehicle and  $N$  the number of vehicles present during the measurement. The mean speed computed by the previous equations, is called the *average travel speed* (the computation also includes stopped vehicles), which is more commonly known as the *space-mean speed* (SMS); we denote it with  $\bar{v}_s$  (note that in some engineering disciplines, the sole letter  $u$  is used to denote a mean speed, however, this is ambiguous in our opinion).

It is interesting to see that the spatial measurement is based on an *arithmetic average* of the vehicles' *instantaneous speeds*, whereas the temporal measurement is based on the *harmonic average* of the vehicles' *spot speeds*. If we instead were to take the arithmetic average of the vehicles' spot speeds in the temporal measurement region  $R_t$ , this would lead to what is called the *time-mean speed* (TMS); we denote it by  $\bar{v}_t$ :

$$\bar{v}_t = \frac{1}{N} \sum_{i=1}^N v_i \quad (\text{region } R_t). \quad (26)$$

Similarly, we can compute the time-mean speed for measurement region  $R_s$ , by taking the harmonic average of the vehicles' instantaneous speeds. With respect to both

space- and time-mean speeds, Wardrop has shown that the following relation holds [115]:

$$\bar{v}_t = \bar{v}_s + \frac{\sigma_s^2}{\bar{v}_s}, \quad (27)$$

with  $\sigma_s^2$  the statistical sample variance defined as follows:

$$\sigma_s^2 = \frac{1}{N-1} \sum_{i=1}^N (v_i - \bar{v}_s)^2, \quad (28)$$

in which  $v_i$  denotes the  $i^{\text{th}}$  vehicle's instantaneous speed. One of the main consequences of equation (27), is that the time-mean speed always exceeds the space-mean speed (except when all the vehicles' speeds are the same, in which case the sample variance is zero and, as a consequence, the time- and space-mean speeds are equal). So a stationary observer will most likely see more faster than slower vehicles passing by, as opposed to e.g., an aerial photograph in which more slower than faster vehicles will be seen [27]. Despite this mathematical quirk, the practical difference between SMS and TMS is often negligible for free-flow traffic (i.e., light traffic conditions); however, under congested traffic conditions both mean speeds will behave substantially differently (i.e., around 10%).

Using equation (27), we can also estimate the space-mean speed, based on the time-mean speed and approximating the variance of the SMS with that of the TMS [9]:

$$\begin{aligned} \bar{v}_s &= \bar{v}_t - \frac{\sigma_s^2}{\bar{v}_s}, \\ &\approx \bar{v}_t - \frac{\sigma_t^2}{\bar{v}_s}, \\ &\Downarrow \\ \bar{v}_s - \bar{v}_t &\approx -\frac{\sigma_t^2}{\bar{v}_s}, \\ \bar{v}_s^2 - \bar{v}_s \bar{v}_t &\approx -\sigma_t^2, \\ \bar{v}_s^2 - 2\bar{v}_s \frac{\bar{v}_t}{2} + \frac{\bar{v}_t^2}{4} &\approx \frac{\bar{v}_t^2}{4} - \sigma_t^2, \\ \left(\bar{v}_s - \frac{\bar{v}_t}{2}\right)^2 &\approx \frac{\bar{v}_t^2}{4} - \sigma_t^2, \\ &\Downarrow \\ \bar{v}_s &\approx \frac{\bar{v}_t}{2} + \sqrt{\frac{\bar{v}_t^2}{4} - \sigma_t^2} \quad \forall \bar{v}_t \geq 2\sigma_t \end{aligned} \quad (29)$$

In general, using the space-mean speed is preferred to the time-mean speed. However, in most cases only this latter traffic flow characteristic is available, so care should be taken when interpreting the results of a study (unless of course when SMS and TMS are negligibly different).

The extension of equation (25) to multi-lane is straightforward; for example, the space-mean speed is computed

as follows:

$$\bar{v}_s = \begin{cases} \frac{\sum_{l=1}^L \sum_{i=1}^{N_l} v_{i,l}}{\sum_{l=1}^L N_l} & \text{(region } R_s), \\ \frac{1}{\frac{1}{L} \sum_{l=1}^L \frac{1}{\sum_{i=1}^{N_l} v_{i,l}}} & \text{(region } R_t), \end{cases} \quad (30)$$

with now  $v_{i,l}$  the instantaneous (or spot) speed of the  $i^{\text{th}}$  vehicle in lane  $l$ .

## 2. Fundamental relation of traffic flow theory

There exists a unique relation between three of the previously discussed macroscopic traffic flow characteristics density  $k$ , flow  $q$ , and space-mean speed  $\bar{v}_s$  [115]:

$$q = k \bar{v}_s. \quad (31)$$

This relation is also called the *fundamental relation of traffic flow theory*, as it provides a close bond between the three quantities: knowing two of them allows us to calculate the third one (note that the time-mean speed in equation (26) does not obey this relation). In general however, there are two restrictions, i.e., the relation is only valid for (1) continuous variables[124], or smooth approximations of them, and (2) traffic composed of substreams (e.g., slow and fast vehicles) which comply to the following two assumptions:

### Homogeneous traffic

There is a homogeneous composition of the traffic substream (i.e., the same type of vehicles).

### Stationary traffic

When observing the traffic substream at different times and locations, it 'looks the same'. Putting it a bit more quantitatively, all the vehicles' trajectories should be parallel and equidistant [27]. A stationary time period can be seen in a cumulative plot (e.g., Fig. 4) where the curve corresponds to a linear function.

The latter of the above two conditions, is also referred to as traffic operating in a *steady state* or at *equilibrium*. Based on equations (5) and (12) using partial densities and flows for different substreams (e.g., vehicle classes with distinct travel speeds, macroscopic characteristics of different lanes, ...), we can now calculate the space-mean speed, using relation (31), in the following equivalent ways:

$$\begin{aligned}\bar{v}_s &= q / k, \\ &= \sum_{c=1}^C q_c / \sum_{c=1}^C k_c, \quad (32)\end{aligned}$$

$$= \sum_{c=1}^C q_c / \sum_{c=1}^C \frac{q_c}{\bar{v}_{s_c}}, \quad (33)$$

$$= \sum_{c=1}^C k_c \bar{v}_{s_c} / \sum_{c=1}^C k_c, \quad (34)$$

in which  $C$  denotes the number of substreams,  $q_c$ ,  $k_c$ ,  $\bar{v}_{s_c}$ , and  $\bar{v}_{t_c}$  the flow, density, space, and time-mean speed respectively of the  $c$ -th substream. In the above derivations, equation (32) should be used when both the flows and densities are known, equation (33) should be used when both the flows and space-mean speeds are known, and equation (34) should be used when both the densities and space-mean speeds are known.

As can be seen in equation (34), the space-mean speed is calculated by averaging the substreams' space-mean speeds using their densities as weighting factors. Similarly, the time-mean speed can be derived by using the flows as weighting factors for the substreams' time-mean speeds:

$$\bar{v}_t = \sum_{c=1}^C q_c \bar{v}_{t_c} / \sum_{c=1}^C q_c, \quad (35)$$

Because density can not always be easily measured, we can compute it using the fundamental relation (31). Density can then be directly derived from flow and space-mean speed measurements, or if the latter are not available, they can be estimated from occupancy measurements; in [20, 21, 22], Coifman provides a nice set of techniques for dealing with these difficulties.

### E. Moving observer method and floating car data

When measuring and/or computing the macroscopic traffic flow characteristics in the previous sections, we always assumed a fixed measurement region. There exists however yet another method, based on what is called a *moving observer* [116]. The idea behind the technique is to have a vehicle drive in both directions of a traffic flow, each time recording the number of oncoming vehicles and the net number of vehicles it gets overtaken by, as well as the times necessary to complete the two trips. Note that the assumption of stationary traffic still has to hold, i.e., the round trip should be completed before traffic conditions change significantly.

Using this method, it is then possible to derive the flow and density of the traffic stream in the direction of interest [27, 39]. However, the main disadvantage of this method is that, in order to obtain an acceptable level of accuracy

on a road with a low flow, a very large number of trips are required [39, 84, 116].

One of the techniques that has entered the picture during the last decade, is the use of so-called *floating cars* or *probe vehicles*. They can be compared to the moving observer method, but in this case, the vehicles are equipped with GPS and GSM(C)/GPRS devices that determine their locations based on the USA's NAVSTAR-GPS (or Europe's planned GNSS Galileo), and transmit this information to some operator. Initially, this allows an agency, e.g., a parcel delivery service, to track its vehicles throughout a network, based on their locations. Nowadays, the technique has evolved, resulting in several completed field tests of which the main goal was to estimate the traffic conditions based on a small number of probe vehicles. During field measurements, floating cars can mimic several types of behaviour, most notably by travelling at the traffic flows' mean speed, or by trying to travel at the road's speed limit, or even by chasing another randomly selected vehicle from the traffic stream.

Some examples of studies and experiments with floating car data (FCD) are given in the following. Firstly, Fastenrath gives an overview of a telematic field trial (*VEhicle Relayed Dynamic Information*, VERDI) that addresses issues such as economical, political, and technical constraints [38]. Secondly, Westerman provides an overview of available techniques for obtaining real-time road traffic information, with the goal of controlling the traffic flows through telematics [118], and Wermuth et al. describe a 'TeleTravel System' used for surveying individual travel behaviour [117]. Then, Taale et al. compare travel times from floating car data with measured travel times (using a fleet of sixty equipped vehicles driving around in Rotterdam, The Netherlands), concluding that they correspond reasonably well [107]. Next, Michler derives the minimum percentage of vehicles necessary, in order to estimate traffic stream characteristics for certain traffic patterns (e.g., free-flow and congested traffic) based on rigid statistical grounds [81], and Linauer and Leihls measure the travel time between points in a road network, based on a high number of users that submit a low number of GSM hand-over messages [73]. In addition, Demir et al. accurately reconstruct link travel times during periods of traffic congestion, using only a very limited number of FCD-messages with a small number of users [33]. A final, more regional, example is the founding of the government-supported Belgian 'Telematics Cluster'[125], a platform for encouraging the use of telematics solutions for ITS. The initiative already includes some 57 members, stimulating the cooperation between users, telecommunication companies, and the automotive industry.

In conclusion, we can state that the use of probe vehicles provides an effective way to gather accurate current travel times in a road network, thereby allowing good up-to-date estimations of traffic conditions. The technique will continue to grow and evolve, already by introducing personalised traffic information to drivers, based on their location and the surrounding traffic conditions. This development is furthermore stimulated by the fact that GSM market penetration still rises above 70% [73], and

it is our belief this will also be the case for personal GPS devices and in-vehicle route planners.

Despite the obvious major advantage of obtaining accurate information on the traffic conditions, the technique suffers from a jurisprudential battle, in that there are many delicately privacy concerns involved with respect to the mobile operator that wants to track individual people's units (not to mention the monetary cost associated with the numerous induced communications).

#### IV. PERFORMANCE INDICATORS

After considering the previously mentioned macroscopic traffic flow characteristics, we now take a look at some popular performance indicators used by traffic engineers when assessing the quality of traffic operations. We concisely discuss the peak hour factor, the reliability of travel times, the levels of service, and a measure of efficiency of a road. For a more complete overview, we refer the reader to [105].

##### A. Peak hour factor

During high flow periods in the peak hour, a possible indicator for traffic flow fluctuations is the so-called *peak hour factor* (PHF). It is calculated for one day as the average flow during the hour with the maximum flow, divided by the peak flow rate during one quarter hour within this hour [79]:

$$\text{PHF} = \frac{\bar{q}_{160}}{\bar{q}_{15}}. \quad (36)$$

For example, suppose we measure flows on a main unidirectional road with three lanes, during a morning peak: from 07:00 to 08:00 we measure consecutively 3500, 6600, 6200, and 4500 vehicles/hour during each quarter. The total average flow  $\bar{q}_{160}$  is 5200 vehicles/hour, with a peak 15 minute flow rate  $\bar{q}_{15} = 6600$  vehicles/hour. The PHF is therefore equal to  $5200/6600 = 0.78$ .

Note that some manuals express the peak 15 minute flow rate as the number of vehicles during that quarter hour, necessitating an extra multiplication by 4 in the denominator of equation (36) to convert the flow rate to an hourly rate.

We can immediately see that the PHF is constrained to the interval  $[0.25, 1.00]$ ; the higher the PHF, the flatter the peak period (i.e., a longer sustained state of high flow). Typically, the PHF has values around 0.7 – 0.98. Note that two of the obvious problems with the PHF are, on the one hand, the question of when to pick the correct 15 minute interval, and on the other hand the fact that some peak periods may last longer than one hour.

##### B. Travel times and their reliability

When travelling around, people like to know how long a specific journey will take (e.g., by public transport, car, bicycle, ...). This notion of an expected travel time, is one of the most tangible aspects of journeying as perceived by the travellers. When people are travelling to their work, they are required to arrive on time at their destinations. Based on this premise, we can naturally state that people reason with a built-in safety margin: they consider the *average time* it takes to reach a destination, and use this to decide about their departure time.

Aside from the above obvious human rationale, there is also an increased interest in obtaining precise information with respect to travel times in the context of *advanced traveller information systems* (ATIS). Here, an essential ingredient is the accurate prediction of future travel times. Coupled with incident detection for example, drivers can obtain correct travel time information, thereby staying informed of the actual traffic conditions and possibly changing their journey. The requested information can reach the driver by means of a cell-phone (e.g., as a feature offered by the mobile service provider), it can be broadcasted over radio (e.g., the *Traffic Message Channel* – TMC), or it can be displayed using *variable message signs* (VMS) above certain road sections (e.g., *dynamic route information panels* – DRIPs), ...

##### 1. Travel time definitions

The travel time of a driver completing a journey, can be defined as ‘the time necessary to traverse a route between any two points of interest’ [111]. In this context, the *experienced dynamic travel time*, starting at a certain time  $t_0$ , over a road section of length  $K$  is defined as follows [9]:

$$T(t_0) = \int_0^K \frac{1}{v(t, x)} dx \quad \forall t \geq t_0, \quad (37)$$

for which it is assumed that all local *instantaneous* vehicle speeds  $v(t, x)$  are known at all points along the route, and at all time instants (hence the term *dynamic* travel time). In most cases however, we do not know all the  $v(t, x)$ , but only a finite subset of them, defined by the locations of the detector stations (demarcating section boundaries). The travel time can then be approximated using the recorded speeds at the beginning and end of a section (there is an underlying assumption here, namely that vehicles travel at a more or less constant speed between detector locations). As stated earlier, the experienced travel time requires the knowledge of local vehicle speeds at *all* time instants after  $T_0$ . Because this is not always possible, a simplification can be used, resulting in the so-called *experienced instantaneous travel time*:

$$\tilde{T}(t_0) = \int_0^K \frac{1}{v(t_0, x)} dx, \quad (38)$$

In general, we can derive the travel time using equation (25), i.e., the total distance travelled by all the vehicles, divided by their space-mean speed:

$$T(t_0) = \frac{K}{\bar{v}_s(t_0)}, \quad (39)$$

in which an accurate estimation of the space-mean speed  $\bar{v}_s(t_0)$  at time  $t_0$  is necessary (e.g., by taking the harmonic average of the recorded spot speeds).

## 2. Queueing delays

Traffic congestion nearly always leads to the build up of queues, introducing an increase (i.e., the *delay*) in the experienced travel time. The congestion itself can have originated due to traffic demand exceeding the capacity, or because an incident occurred (e.g., road works, a traffic accident, ...) [126]. This can create *incidental* (non-recurrent) or *structural* (recurrent) congestion. Congestion can thus be seen as a loss in travel time with respect to some base line reference. Two such commonly used references are the travel time under free-flow conditions, and the travel time under maximum (i.e., capacity) flow. The delay is typically expressed in vehicle hours. As stated earlier, there are several ways to inform a driver of the current and predicted travel time. Using DRIPs it is possible to advertise the extra travel time (the delay is now typically expressed in vehicle minutes), as well as queue lengths. We note that in our opinion it is more intuitive to advertise a temporal estimation (i.e., the travel time or the delay), than a spatial estimation (e.g., the queue length on a motorway).

## 3. An example of travel time estimation using cumulative plots

There exist several techniques for estimating the current travel time; one method for directly ‘measuring’ the travel time, is by using a probe vehicle (we refer the reader to section III E for more details). This way, it is possible to extract actual travel times from a traffic stream. Note that as traffic conditions get more congested, more probe vehicles are required in order to obtain an accurate estimation of the travel time.

Another method for measuring the travel time, is based on historical data, namely cumulative plots (introduced in section III B 2). As mentioned earlier, the travel time can then be measured as the distance along the horizontal (or oblique) time axis; any excess due to delays can then easily be spotted on a set of oblique cumulative plots.

Based on cumulative plots of consecutive detector stations, we can calculate the travel time between the upstream and downstream end of a road section. To illustrate this, let us reconsider the cumulative curves shown in Fig. 4 of section III B 2. The evolution of the travel

time during the day for these curves, is depicted in the top part of Fig. 5. The derived histogram (indicative of the underlying travel time probability density function), in the bottom part of the figure, shows that the mean travel time during the day is approximately 4 minutes.

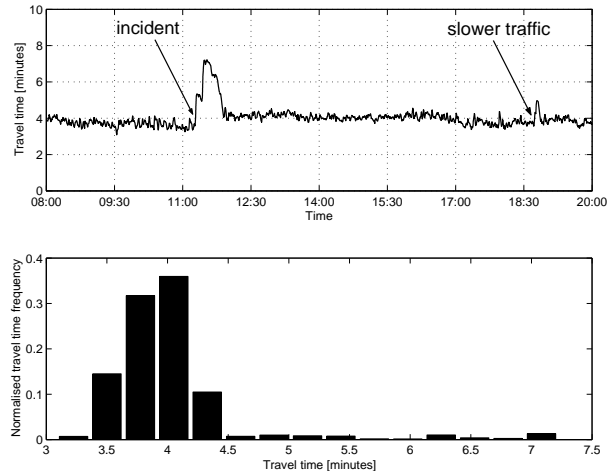


FIG. 5: *Top*: The evolution of the travel time during one day, based on the cumulative plots from section III B 2. As can be seen, an incident likely occurred at 11:00, increasing the travel time from 4 to 7 minutes. Furthermore, at approximately 18:45 in the evening, all traffic seemed to simultaneously slow down for a period of some 10 minutes. *Bottom*: Based on the calculated travel times during the day, we can derive a histogram that is an approximation of the underlying travel time probability density function. The mean is located around 4 minutes.

We already mentioned the likely occurrence of an incident at 11:00, resulting in the formation of a queue. During this period, the travel time shot up, reaching first 5, then 7 minutes. Looking at the top part of Fig. 5, we furthermore notice a slight increase in the travel time at approximately 18:45, for a short period of some 10 minutes. Investigation of the detector data, revealed that the flow remained constant at about 4500 vehicles per hour, but the speed dropped to some 90 km/h (as opposed to 110 km/h); we can conclude that all vehicles were probably simultaneously slowing down during this period (perhaps a rubbernecking effect). Another possibility is a platoon of slower moving vehicles, but then it would seem to have dissipated rather quickly after 10 minutes.

Using ample historical data, we can analyse the travel time over a period of many weeks, months, or even years. This would allow us to make *intuitive* statements such as:

*“The typical travel time over this section of the road during a working Monday, lies approximately between 4 and 6 minutes. There is however an 8% probability that the travel time increases to some 22 minutes (e.g., due to an occurring incident).”*

Finally note that, besides the two previously mentioned techniques for estimating travel times, an extensive overview can be found in the *Travel Time Data Collection Handbook* [11]. Another concise but more theoretically-oriented overview is provided by Bovy and Thijs [9].

As mentioned in the introduction of this section, people reason about their expected travel times based on a built-in safety margin. Central to this is the concept of the *average travel time*. The *reliability* of such a travel time is then characterised by its *standard deviation*. Drivers typically accept (and sometimes expect) a small delay in their expected travel time. A traveller knows the *expected travel time* because of the familiarity with the associated trip. To the traveller, this is personal historical information, for instance obtained by learning the trip’s details (e.g., the traffic conditions during a typical morning rush hour) [5].

Directly linked to the reliability of a certain expected travel time, is its variability. They are said to be unreliable when both expected and experienced travel times differ sufficiently. A typical characterisation of reliability involves the mean and standard deviation (i.e., the variance, which is a measure of variability) of a travel time distribution [19]. An example of such a travel time distribution for one day is shown in the histogram in the bottom part of Fig. 5.

Both first- and second-order measures of a distribution are by themselves insufficient to capture the complete picture. In order to grasp the notion of the previously mentioned safety margin, another typical statistical measure is considered, namely the *90<sup>th</sup> percentile*. The rationale behind the use of this percentile is that travellers adopt a certain ‘safe’ threshold with respect to their expected journey times. Considering the 90<sup>th</sup> percentile, this means that only one out of ten times the experienced travel time will differ significantly from the expected travel time. Travel time reliability can thus be viewed upon as a measure of service quality (similar to the concept of ‘quality of service’ (QoS) in telecommunications).

There has been some research into the analytic form of travel time distributions (e.g., the work of Arroyo and Kornhauser, concluding that a lognormal distribution seems the most appropriate [4]). There exist however significant differences between travel time distributions: in general, a smaller standard deviation indicates a better service quality and reliability. In contrast to this, a large standard deviation is indicative of chaotic behaviour of the traffic flow, the latter being totally unstable. Furthermore, travel time distributions can have a long tail; this signifies seldom events (e.g., incidents), that can have significant repercussions on the quality of traffic operations.

Let us finally note that there is an increased interest in the *reliability of complete transportation networks*, and their *robustness* against incidents. To this end, Immers et al. consider reliability as a user-oriented quality, whereas robustness is more a property of the system itself [51]. Among several characterising factors for robustness of transportation systems, they also introduce the following practical notions in this context: *redundancy*, denoting a spare capacity, and *resilience*, which is the ability to repeatedly recover from a temporary overload. Their conclusion is that the key element in securing transportation reliability lies in a good network design.

### C. Level of service

Historically, one of the main performance indicators to assess the quality of traffic operations, was the *level of service* (LOS), introduced in the 1960s. It is represented as a grading system using one of six letters (A – F), whereby LOS A denotes the best operating conditions and LOS F the worst. These LOS measures are based on road characteristics such as speed, travel time, . . . , and drivers’ perceptions of comfort, convenience, . . . [1]. As is customary among traffic engineers, these representative statistics of these characteristics are collectively called *measures of effectiveness* (MOE).

Levels A through D are representative for free-flow conditions whereby LOS A corresponds to free flow, LOS B to reasonable free flow, LOS C to stable traffic operations, and LOS D to bordering unstable traffic operations. LOS E is reminiscent of near-capacity flow conditions that are extremely unstable, whereas LOS F corresponds to congested flow conditions (caused by either structural or incidental congestion) [79].

As an example, we provide an overview of the different levels of service in Table I (based on [79], in similar form originally published in the *Highway Capacity Manual* (HCM) of 1985 as the *Transportation Research Board’s* (TRB)[127] special report #209.

LOS	Density (veh/km)	Occupancy (%)	Speed (km/h)
A	0 → 7	0 → 5	≥ 97
B	7 → 12	5 → 8	≥ 92
C	12 → 19	8 → 12	≥ 87
D	19 → 26	12 → 17	≥ 74
E	26 → 42	17 → 28	≥ 48
F	42 → 62 > 62	28 → 42 > 42	< 48

TABLE I: Level of service (LOS) indicators for a motorway (adapted from [79], in similar form originally published in the 1985 HCM).

Calculating levels of service can be done using a multitude of methods; some examples include using the density (at motorways), using the space-mean speed (at arterial streets), using the delay (at signalled and unsignalled intersections), . . . [1]. The distinction

between different LOS is primarily based on the measured average speed, and secondly on the density (or occupancy). Furthermore, as traditional analyses only focus on a select number of hours, a new trend is to conduct *whole year analyses* (WYA) based on aggregated measurements such as e.g., the *monthly average daily traffic* (MADT) and the *annual average daily traffic* (AADT) [10]. The MADT is calculated as the average amount of traffic recorded during each day of the week, averaged over all days within a month. Averaging the resulting twelve MADTs gives the AADT.

Regarding the use of the LOS, we note that it is a rather old-fashioned method for evaluating the quality of traffic operations. In general, it is difficult to calculate, mainly because the defined standards at which the different levels are set, always depend on the specific type of traffic situation that is studied (e.g., type of road, . . .). This makes the LOS more of an engineering tool, used when assessing and planning operational analyses. Instead of using the LOS, we therefore propose to adopt the more suited approach based on oblique cumulative plots (we refer the reader to section III B 2). These allow for example to assess the differences between travel times under free-flow and congested conditions, thereby giving a more meaningful and intuitive indication of the quality of traffic operations to the drivers.

#### D. Efficiency

In [18], Chen et al. state that the main reason for congestion is not demand exceeding capacity (i.e., the number of travellers who *want* to use a certain part of the transportation network, exceeds the available infrastructure's capacity), but is in fact the inefficient operation of motorways during periods of high demand. In order to quantify this efficiency, they first look at what the prevailing speed is when a motorway is operating at its maximum efficiency, i.e., the highest flow (corresponding to the effective capacity, which is different from the HCM's capacity which is calculated from the road's physical characteristics). Based on the distribution of 5-minute data samples from some 3300 detectors, they investigate the speed during periods of very high flows. This leads them to a so-called sustained speed  $\bar{v}_{\text{sust}} = 60$  miles per hour (which corresponds to  $60 \text{ mi/h} \times 1.609 \approx 97 \text{ km/h}$ ).

The performance indicator they propose, is called the *efficiency*  $\eta$  and it based on the ratio of the *total vehicle miles travelled* (VMT), divided by the *total vehicle hours travelled* (VHT). Note that as the units of VMT and  $v_{\text{sust}}$  should correspond to each other, we propose to use the terminology of *total vehicle distance travelled* (VDT) instead of the VMT, in order to eliminate possible confusion. Both VDT and VHT are defined as follows:

$$\text{VDT} = q K, \quad (40)$$

$$\text{VHT} = \frac{\text{VDT}}{\bar{v}_s}, \quad (41)$$

with, as before,  $q$  the flow,  $K$  the length of the road section, and  $\bar{v}_s$  the space-mean speed. Using the above definitions, we can write the efficiency of a road section as:

$$\eta = \frac{\text{VDT}/\text{VHT}}{\bar{v}_{\text{sust}}}. \quad (42)$$

The efficiency is expressed as a percentage, and it can rise above 100% when the recorded average speeds surpass the sustained speed  $\bar{v}_{\text{sust}}$ . In general, the discussed efficiency can also easily be calculated for a complete road network and an arbitrary time period. It can furthermore be seen as the ratio of the actual productivity of a road section (the *output* produced by this section during one hour), to its maximum possible production (the *input* to the section) under high flow conditions.

Note that as a solution to their original claim ("*congestion arises due to inefficient operation*"), Chen et al. propose to increase the operational efficiency, mainly through the technique of suitable ramp metering (using an idealised ramp metering control practice that maintains the occupancy downstream of an on ramp to its critical level). But in our opinion, they neglect to take into account the entire situation, i.e., they fail to consider the extra effects induced by holding vehicles back at some on ramps (e.g., the total time travelled by *all* the vehicles, including delays), thus rendering their statement practically worthless by giving a feeble argument. Careful examination of their reasoning, reveals that these extra effects are dealt with by shifting demand during the peak periods. . . but this just confirms our hypothesis that congestion occurs when demand exceeds capacity, even when this capacity is for example controlled through ramp metering !

In contrast to the work of Chen et al., Brilon proposes another definition for the *efficiency* (now denoted as  $E$ ): it is expressed as the number of vehicle kilometres that are produced by a motorway section per unit of time [10]:

$$E = q \bar{v}_s T_{\text{mp}}, \quad (43)$$

with now  $q$  the total flow recorded during the time interval  $T_{\text{mp}}$ . Brilon concludes that in order for motorways to operate at maximum efficiency, their hourly flows typically have to remain *below* the capacity flow (e.g., at 90% of  $q_{\text{cap}}$ ). Brilon also proposes to use this point of maximum efficiency as the threshold when going from LOS D to LOS E.

Whereas the previous sections dealt with individual traffic flow characteristics, this section discusses some of the relations between them. We first give some characterisations of different traffic flow conditions and the rudimentary transitions between them, followed by a discussion of the relations (which are expressed as fundamental diagrams) between the traffic flow characteristics, giving special attention to the different points of view adopted by traffic engineers.

### A. Traffic flow regimes

Considering a stream of traffic flow, we can distinguish different types of operational characteristics, called *regimes* (two other commonly used terms are traffic flow *phases* and *states*). As each of these regimes is characterised by a certain set of unique properties, classification of them is sometimes based on occupancy measurements (see for example the discussion about levels of service in section IV C), or it is based on combinations of different macroscopic traffic flow characteristics (e.g., the work of Kerner [55]).

In the following sections, we discuss the regimes known as *free-flow* traffic, *capacity-flow* traffic, *congested*, *stop-and-go*, and *jammed* traffic. Our discussion of these regimes is in fact based on the commonly adopted way of looking at traffic flows, as opposed to for example Kerner's three-phase traffic theory that includes a regime known as *synchronised* traffic (we refer the reader to section V D for more details). We conclude the section with a note on the transitions that occur from one regime to another.

#### 1. Free-flow traffic

Under light traffic conditions, vehicles are able to freely travel at their desired speed. As they are largely unimpeded by other vehicles, drivers strive to attain their own comfortable travelling speed (we assume that in case a vehicle encounters a slower moving vehicle ahead, it can easily change lanes in order to overtake the slower vehicle). Notwithstanding this ability for unconstrained travelling, drivers have to take into account the maximum allowed speed (denoted by  $v_{\max}$ ), as well as road-, engine-, and other vehicle characteristics. Note that in some cases, depending on the country under scrutiny, drivers perform speeding.

In essence, the previous description of *free-flow traffic* considers a traffic flow to be unrestricted, i.e., no significant delays are introduced due to possible overtaking manoeuvres. As a consequence, the *free-flow speed* (by some called the *nominal speed*) is the mean speed of all vehicles, travelling at their own pace (e.g., 100 km/h); it is denoted by  $\bar{v}_{\text{ff}}$ .

Free-flow traffic occurs exclusively at low densities, implying large average space headways according to equation (10). As a result, small local disturbances in the temporal and spatial patterns of the traffic stream have no significant effects, hence traffic flow is *stable* in the free-flow regime.

#### 2. Capacity-flow traffic

When the traffic density increases, vehicles are driving closer to each other. Considering the number of vehicles that pass a certain location alongside the road, an observer will notice an increase in the flow. At a certain moment, the flow will reach a maximum value (which is determined by the mean speed of the traffic stream and the current density). This maximum flow is called the *capacity flow*, denoted by  $q_c$ ,  $q_{\text{cap}}$ , or even  $q_{\max}$ . A typical value for the capacity flow on a three-lane Belgian motorway with  $v_{\max}$  equal to 120 km/h, can reach a maximum of some 7000 vehicles [113]. According to equation (17), the average time headway is minimal at capacity-flow traffic, indicating the (local) formation of tightly packed clusters of vehicles (i.e., platoons), which are moving at a certain *capacity-flow speed*  $\bar{v}_c$  (or  $\bar{v}_{\text{cap}}$ ) which is normally a bit lower than the free-flow speed. Note that some of these fast platoons are very unstable when they are composed of tail-gating vehicles: whenever in such a string a vehicle slows down a little, it can have a cascading effect, leading to exaggerate braking of following vehicles. Hence, these latter manoeuvres can destroy the local state of capacity-flow, and can in the worst case lead to multiple rear-end collisions. At this point, traffic becomes *unstable*.

The calculation of the capacity flow is a daunting task, holding traffic engineers occupied for the last six decades. The fact of the matter is that there exists no rigorous definition for the concept of 'capacity'. As a result, after many years of research, this culminated in the publication of the fourth edition of the already previously mentioned *Highway Capacity Manual*. It contains an impressive overview, spanning methodologies for assessing the capacity at specific types of road infrastructures (motorway facilities, weaving sections, on- and off-ramps, signalised and unsignalised urban intersections, ...) [1].

#### 3. Congested, stop-and-go, and jammed traffic

Considering the regime of capacity-flow traffic, it is reasonable to assume that drivers are more mentally aware and alert in this regime, as they have to adapt their driving style to the smaller space and time headways under high speeds. However, when more vehicles are present, the density is increased even further, allowing a sufficiently large disturbance to take place. For example, a driver with too small space and time headways, will have to brake in order to avoid a collision with the leader directly



in front; this can lead to a local chain of reactions that disrupts the traffic stream and triggers a breakdown of the flow. The resulting state of saturated traffic conditions, is called *congested traffic*. The moderately high density at which this breakdown occurs, is called the *critical density*, and is denoted by  $k_c$  or  $k_{\text{crit}}$  (for a typical motorway, its value lies around 25 vehicles (PCUs) per kilometre per lane, [113]). From this knowledge, we can derive the optimal driving speed for single-lane traffic flows as  $\bar{v}_s = q_{\text{cap}}/k_{\text{crit}} = 2000 \div 25 \approx 85$  km/h.

Higher values for the density indicate almost always a worsening of the traffic conditions; congested traffic can result in *stop-and-go traffic*, whereby vehicles encounter so-called *stop-and-go waves*. These waves require them to slow down severely, or even stop completely. When traffic becomes motionless, the space headway reaches a minimum as all vehicles are standing bumper-to-bumper; this extreme state is called *jammed traffic*. Clearly, there exists a maximum density at which the traffic seems to turn into a ‘parking lot’, called the *jam density* and it is denoted by  $k_j$ ,  $k_{\text{jam}}$ , or  $k_{\text{max}}$ . For a typical motorway, its value lies around 140 vehicles (PCUs) per kilometre per lane [113].

Note that the jam density is typically expressed in vehicles per kilometre. As already stated in the introduction of section III A, density ignores the effects of traffic composition and vehicle lengths. For a typical value of some 140 vehicles/km/lane for the jam density, this means that we express the density by using passenger car units (see section III A 2 for more details). Suppose now for example that an average trailer truck equals 4.5 PCUs, then the jam density would decrease to some  $140 \div 4.5 \approx 31$  trucks for this class of vehicles. *As a consequence, the value of the jam density is different for each vehicle class.*

#### 4. A note on the transitions between different regimes

Streams of traffic flows can be regarded as many-particle systems (e.g., gasses, magnetic spin systems, ...); as they have a large number of degrees of freedom, it is often intractable when it comes to solving them exactly. However, from a physical point of view, these systems can be described in the framework of *statistical physics*, whereby the collective behaviour of their constituents is approximately treated using statistical techniques.

Within this context, the changeover from one traffic regime to another, can be looked upon as a *phase transition*. Within thermodynamics and statistical physics, an *order parameter* is often used to describe the phase transition: when the system shifts from one phase to another (e.g., at a *critical point* for liquid-gas transitions), the order parameter expresses a different qualitative behaviour. Two examples of such an order parameter that is applicable to traffic flows, can be found in Schadschneider et al. who considered nearest neighbour correlations [104], and in Jost and Nagel who devised a measure of inhomogeneity [53] (we refer the reader to our work in [78] for

an example in which they are used and compared when tracking phase transitions).

There exists a difference in which a phase transition can express itself. This difference is designated by the order of the transition; generally speaking, the two most common phase transitions are *first-order* and *second-order transitions*. According to *Ehrendfest’s classification*, first-order transitions have an abrupt, discontinuous change in the order parameter that characterises the transition. In contrast to this, the changeover to the new phase occurs smoothly for second-order transitions [71, 119]. Note that higher-order phase transitions also exist, e.g., in superconducting materials [23].

With respect to the description of regimes in traffic flows, it is commonly agreed that there exists a first-order phase transition when going from the capacity-flow to the congested regime. The point at which this transition occurs, is the critical density. Studying the phase transitions encountered in fluid dynamics, there exists a transition from the *laminar* flow (i.e., a fluid flowing in layers, each moving at a different velocity) to the *turbulent* flow (i.e., the disturbed random and unorganised state in which vortices form). However, the transition here is triggered by an increase in the velocity of the fluid, as opposed to the transition in traffic flows where a change in the density can lead to a cascading instability. In this respect, the analogy for traffic flows holds better when comparing them to gas-liquid transitions. Here free-flow traffic corresponds to a gaseous phase, in which particles are evenly spread out in the system. At the point of the phase transition, liquid droplets will form, coagulating together into bigger droplets. This leads to a state where both gaseous and liquid phases coexist, typically in the form of a big liquid droplet surrounded by gas particles. For even higher densities, particles are so close to each other, and the only remaining state is the liquid phase [37, 52, 53, 54, 68, 93].

In conclusion, we refer the reader to the work of Tampère, where an excellent overview is given, detailing the different traffic flow regimes, their transitions, and mechanisms with respect to jamming behaviour [108].

## B. Correlations between traffic flow characteristics

Whereas the previous sections all treated the macroscopic traffic flow characteristics on an individual basis, this section considers some of the relations between them. We start our discussion with a look at the historic origin of fundamental diagrams, after which we shed some light on the different classical approaches. The section concludes with some considerations with respect to empirical measurements.

### 1. The historic origin of the fundamental diagram

As in many scientific disciplines, the resulting statements and theories are often preceded by an investigation of obtained experimental data, which serves as empirical ev-

idence for them. In this line of reasoning, Greenshields was among the first to provide — as far back as 1935 — a basis for most of the classic work on, what are called, *empirical fundamental diagrams*. In his seminal paper, he sketched a *linear relation between the density and the mean speed*, based on empirically obtained data [44]:

$$\bar{v} = \bar{v}_{\text{ff}} \left( 1 - \frac{k}{k_j} \right). \quad (44)$$

As can be seen from Greenshields' relation, when increasing the density from zero to the jam density  $k_j$ , the mean speed will monotonically decrease from the free-flow speed  $\bar{v}_{\text{ff}}$  to zero (note that we dropped the 's' or 't' subscript from the mean speed, as it is not sure whether or not Greenshields used space- or time-mean speed, respectively). The relation can be understood intuitively, by assuming that drivers will tend to slow down in crowded traffic, because this naturally gives them more time to react to changes (e.g., sudden braking of the lead vehicle). As it is reasonable to assume that the mean speed remains unaffected for very low densities, Greenshields furthermore flattened the upper-left part of the regression line (corresponding to the free-flow speed), although this effect is not incorporated in equation (44).

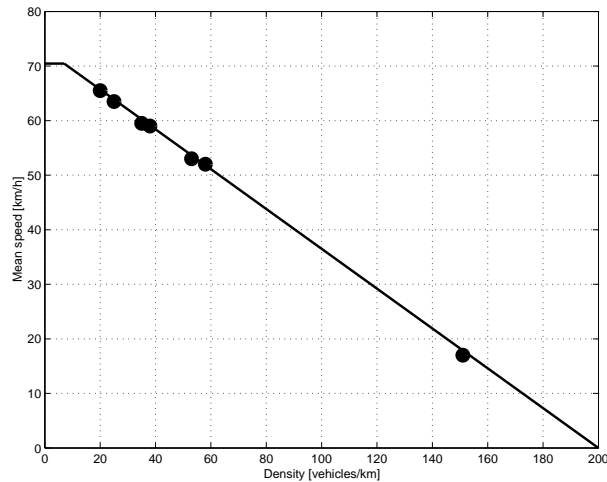


FIG. 6: Greenshields' original linear relation between the density and the mean speed. Note that the regression line is based on only seven measurements points, and that artificial flattening of its upper-left part (figure based on [72] and [39]).

Although Greenshields' derivation of the linear relation between density and space-mean speed appears elegant and simple, it should nevertheless be taken with a grain of salt. The fact of the matter is that his hypothesis is, as can be seen in Fig. 6, based on *only seven measurement points*, which comprise aerial observations taken on September 3rd (Monday, Labor Day), 1934 [79]. One of the problems is that these observations are *not independent*. An even more serious problem is that six of these observations were obtained for free-flow conditions, whereas the one single point that indicates congested

conditions, was obtained at an entirely *different road*, on a *different day* [39] !

Some twenty years later, Lighthill and Whitham developed a theory that describes the traffic flows on long crowded roads using a first-order fluid-dynamic model [72]. As one of the main ingredients in their theory, they postulated the following fundamental hypothesis: “*at any point of the road, the flow  $q$  is a function of the density  $k$* ”. They called this function the *flow-concentration curve* (recall from section III C that density in the past got sometimes referred to as concentration).

Continuing their reasoning, Lighthill and Whitham then referred to Greenshields' earlier work, relating the space-mean speed to the density, and, by means of equation (31), thus relating the flow to the density. The *existence* of the concept of the flow-concentration curve mentioned above, was justified on the grounds that it describes traffic operating under steady-state conditions, i.e., homogeneous and stationary traffic as explained in section III D 2. In this context, the flow-concentration curve therefore describes the *average characteristics* of a traffic flow. So Greenshields first fitted a regression line to scarce data, after which his functional form seemed to be taken for granted for the following seventy years. The key aspect in Lighthill and Whitham's (and also Richards' [102]) approach, lay in the fact that they broadened the flow-concentration curve's validity, including also conditions of non-stationary traffic. They also stated that, because of e.g., changes in the traffic composition, the curve can vary from day to day, or even within a day (e.g., rush hours, ...). The same statement holds also true when considering the flow-concentration curves of different vehicle classes (e.g., cars and trucks).

The term *fundamental diagram* itself, is historically based on Lighthill and Whitham's *fundamental hypothesis* of the existence of such a *one-dimensional* flow-concentration curve. As traffic engineers grew accustomed to the graphical representation of this curve, they started talking about the *diagram* that represents it, i.e., the 'fundamental diagram' [45].

In its original form, the fundamental diagram represents an *equilibrium relation* between flow and density, denoted by  $q_e(k)$ . But note that, because of the fundamental relation of traffic flow theory (see section III D 2), is it equally justified to talk about the  $\bar{v}_{s_e}(k)$  or the  $\bar{v}_{s_e}(q)$  fundamental diagrams. Due to this equilibrium property, the traffic states (i.e., the density, flow, and space-mean speed) can be thought of as 'moving' over the fundamental diagrams' curves.

## 2. The general shape of a fundamental diagram

We now give an overview of some of the qualitative features of the different possible fundamental diagrams, representing the equilibrium relations between density,

space-mean speed, and average space headway, and flow. Note that in each example, we consider a *possible* fundamental diagram, as they can take on many (functional) shapes.

### Space-mean speed versus density

We start our discussion based on the equilibrium relation between space-mean speed and density, i.e., the  $\bar{v}_{s_e}(k)$  fundamental diagram. The main reason for starting here, is the fact that this diagram is the easiest to understand intuitively. Complementary to the example of Greenshields in Fig. 6, we give a small overview of its most prominent features:

- the density is restricted between 0 and the maximum density, i.e., the jam density  $k_j$ ,
- the space-mean speed is restricted between 0 and the maximum average speed, i.e., the free-flow speed  $\bar{v}_{ff}$ ,
- as density increases, the space-mean speed monotonically decreases,
- there exists a small range of low densities, in which the space-mean speed remains unaffected and corresponds more or less to the free-flow speed,
- and finally, the flow (equal to density times space-mean speed), can be derived as the area demarcated by a rectangle whose lower-left and upper-right corners are the origin and a point on the fundamental diagram, respectively.

### Space-mean speed versus average space headway

Microscopic and macroscopic traffic flow characteristics are related to each other by means of equations (10) and (17). According to the former, density  $k$  is inversely proportional to the average space headway  $\bar{h}_s$ . We can therefore derive a fundamental diagram, similar to the previous one, by substituting the density with the average space headway. As a result, the abscissa gets ‘inverted’, resulting in the fundamental diagram as shown in Fig. 7.

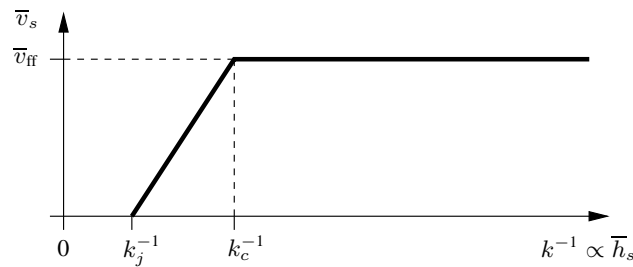


FIG. 7: A fundamental diagram relating the average space headway  $\bar{h}_s$  to the space-mean speed  $\bar{v}_s$ . Note that the average space headway is proportional to the inverse of the density, i.e.,  $k^{-1}$ .

The interesting features of this type of fundamental diagram, can be summed as follows:

- the curve starts not in the origin, but at  $k_j^{-1}$ , corresponding to the average space headway when the

jam density is reached (i.e., all vehicles are standing nearly bumper to bumper),

- as the average space headway increases, its inverse (the density) decreases, and the space-mean speed increases,
- the space-mean speed continues to rise with an increasing average space headway, until it reaches the maximum average speed, i.e., the free-flow speed  $\bar{v}_{ff}$ ; this happens at the inverse of the critical density  $k_c^{-1}$ ,
- from then on, the space-mean speed remains constant with increasing average space headway.

The above features can be understood intuitively: at large average space headways, a driver experiences no influence from its direct frontal leader. However, there exists a point at which the driver comes ‘close enough’ to this leader (i.e., in crowded traffic), so that its speed will decrease. This slowing down will continue to persist as traffic gets more dense (this is the same reasoning behind Greenshields’ derivation in section V B 1).

### Flow versus density

Probably the most encountered form of a fundamental diagram, is that of flow versus density. Its origins date back to the seminal work of Lighthill and Whitham who, as described earlier, referred to it as the flow-concentration curve. An example of the  $q_e(k)$  fundamental diagram is depicted in Fig. 8.

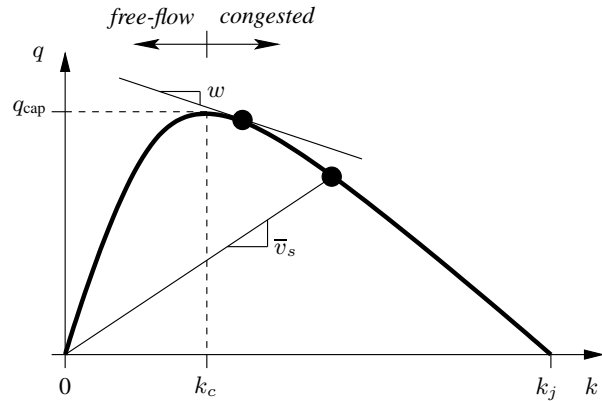


FIG. 8: A fundamental diagram relating the density  $k$  to the flow  $q$ . The capacity flow  $q_{cap}$  is reached at the critical density  $k_c$ . The space-mean speed  $\bar{v}_s$  for any point on the curve, is defined as the slope of the line through that point and the origin. Taking the slope of the tangent to points on the curve, gives the characteristic wave speed  $w$ .

Noteworthy features of this type of fundamental diagram are:

- for moderately low densities (i.e., below the critical density  $k_c$ ), the flow increases more or less linearly (this is called the *free-flow branch* of the fundamental diagram),

- near the critical density  $k_c$ , the fundamental diagram can bend slightly, due to faster vehicles being obstructed by slower vehicles, thereby lowering the free-flow speed [97],
- at the critical density  $k_c$ , the flow reaches a maximum, called the capacity flow [128]  $q_{\text{cap}}$ ,
- in the congested regime (i.e., for densities higher than the critical density), the flow starts to degrade with increasing density, until the jam density  $k_j$  is reached and traffic comes to a stand still, resulting in a zero flow (this is called the *congested branch* of the fundamental diagram),
- the space-mean speed  $\bar{v}_s$  for any point on the  $q_e(k)$  fundamental diagram, can be found as the slope of the line through that point and the origin,

There is one more piece of information revealed by the  $q_e(k)$  fundamental diagram: When taking the slope of the tangent in any point of the diagram, we obtain what is called the *kinematic wave speed*. These speeds  $w$  correspond to *shock waves* encountered in traffic flows (e.g., the stop-and-go waves). As can be seen from the figure, the shock waves travel forwards, i.e., *downstream*, in free-flow traffic ( $w \geq 0$ ), but backwards, i.e., *upstream*, in congested traffic ( $w \leq 0$ ).

The above shape of the  $q_e(k)$  fundamental diagram is just one possibility. There exist many different flavours, originally derived by traffic engineers seeking a better fit of these curves to empirical data. After the work of Greenshields, another functional form — based on a logarithm — was proposed by Greenberg [43]. Another possible form was introduced by Underwood [112]. All of the previous diagrams are called *single-regime models*, because they formulate only one relation between the macroscopic traffic flow characteristics for the entire range of densities (i.e., traffic flow regimes) [79]. In contrast to this, Edie started developing *multi-regime models*, allowing for discontinuities and a better fit to empirical data coming from different traffic flow regimes [35]. We refer the reader to the work of Drake et al. [34] and the book of May [79] for an extensive comparison and overview of these different modelling approaches (note that Drake et al. used time-mean speed).

During the last two decades, other, sometimes more sophisticated, functional relationships between density and flow have been proposed. Examples are the work of Smulders who created a non-differentiable point at the critical density in a two-regime fundamental diagram [106], the METANET model of Messmer and Papageorgiou who's single-regime fundamental diagram contains an inflection point near the jam density [80], the work of De Romph who generalised Smulders' functional description of his two-regime fundamental diagram [103], the typical triangular shape of the fundamental diagram introduced by Newell, resulting in only two possible values for the kinematic wave speed  $w$  [97], ... As can be seen, these fundamental diagrams sometimes take on non-concave forms, depending on the existence of inflection points in the functional relation between flow

and density. In general, they can be convex, concave, (dis)continuous, piecewise-linear, everywhere differentiable, have inflection points, ... Variations in shape will continue to be proposed, as it is for certain that there is no general consensus among traffic engineers regarding the correct shape of this fundamental diagram. To illustrate this, a more exotic approach is based on *catastrophe theory*, which is, in a sense, a three-dimensional model that jointly treats density, flow, and space-mean speed. Acha-Daza and Hall applied the technique, resulting in a satisfactory fit with empirical data [2].

The most extreme argument with respect to the shape of the fundamental diagram, came from Kerner who questioned its validity, and consequently rejected it altogether by replacing it with his fundamental hypothesis of *three-phase traffic flow theory* (refer to section VD for more details) [55].

### Space-mean speed versus flow

An often spotted shape is that of the  $\bar{v}_{s_e}(q)$  fundamental diagram, depicted in Fig. 9. As opposed to the earlier discussed  $\bar{v}_{s_e}(k)$  fundamental diagram, the space-mean speed versus flow curve no longer embodies a function in the strict mathematical sense: for each value of the flow, there exists two different mean speeds, namely one in the free-flow regime (upper branch) and one in the congested regime (lower branch).

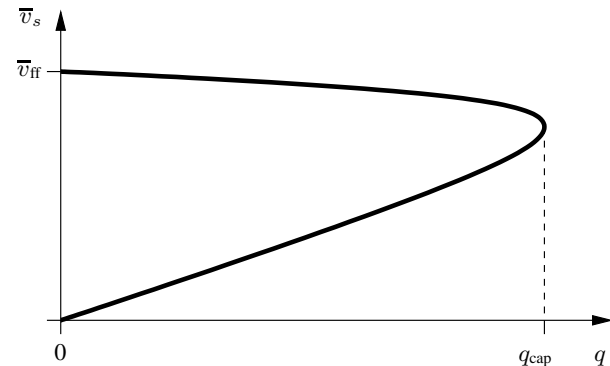


FIG. 9: A fundamental diagram relating the flow  $q$  to the space-mean speed  $\bar{v}_s$ . The capacity flow  $q_{\text{cap}}$  is located at the right edge of the diagram, i.e., it is defined as the maximum average flow. Note that there are two possible speeds associated with each value of the flow.

Some people, e.g., economists who use the flow to represent traffic demand, find this kind of fundamental diagram easy to cope with. But in our opinion, we are convinced however, that this diagram is rather difficult to understand at first sight. We believe the  $\bar{v}_{s_e}(k)$  fundamental diagram is a much better candidate, because density can intuitively be understood as a measure for how crowded traffic is, as opposed to some flow giving rise to two different values for the space-mean speed.

As a final comment, we would like to point out that the previously discussed bivariate functional relationships between the traffic flow characteristics (e.g., density and flow), are based on observations. More importantly, this

means that there is *no direct causal relation* assumed between any two variables. Fundamental diagrams sketch *only possible correlations*, implying that the *nature of the transitions* between different traffic regimes thus remains to be explored (see section V A 4 for a discussion).

### 3. Empirical measurements

As mentioned earlier, the fundamental diagrams discussed in the previous section represent equilibrium relations between the macroscopic traffic flow characteristics of section III. In sharp contrast to this, real empirical measurements from detector stations do not describe such nice one-dimensional curves corresponding to the functional relationships.

As an illustrative example, we provide some scatter plots in Fig. 10. The shown data comprises detector measurements (the sampling interval was one minute) during the entire year 2003; they were obtained by means of a video camera [113] located at the E17 three-lane motorway near Linkeroever[129], Belgium. Because of the nature of this data, we only obtained flows, occupancies, and time-mean speeds. After calculating the average vehicle length, the occupancies were converted into densities using equation (22). Using these recorded time series, we then constructed scatter plots of the density, time-mean speed, flow, and average space headway. Note that no substantial changes are introduced in these plots due to e.g., our using of densities calculated from occupancies, instead of using real measured densities.

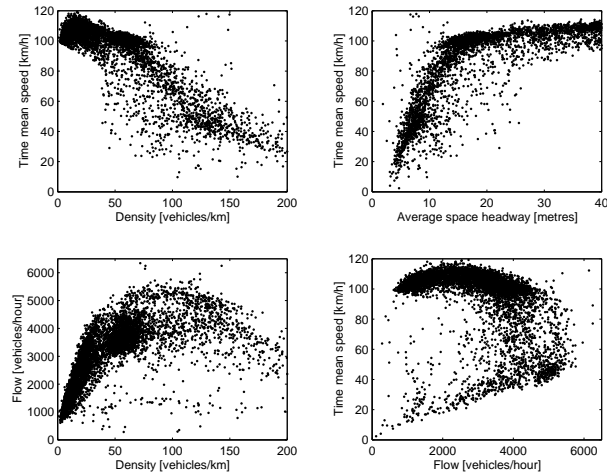


FIG. 10: Illustrative scatter plots of the relations between traffic flow characteristics as measured by video camera CLO3 located at the E17 three-lane motorway near Linkeroever, Belgium. The measured occupancies were converted into densities, the time-mean speed remained unchanged. Shown are scatter plots of a  $(k, \bar{v}_t)$  diagram (top-left), a  $(\bar{h}_s, \bar{v}_t)$  diagram (top-right), a  $(k, q)$  diagram (bottom-left), and a  $(q, \bar{v}_t)$  diagram (bottom-right).

As the dimension of time is removed in these scatter plots, Daganzo calls them *time-independent models* [27]. It is important to understand that *these scatter plots are not fundamental diagrams*, because the latter represent

one-dimensional equilibrium curves. According to Helbing, a better designation would be *regression models* [47]. In this dissertation, we introduce a terminology based on *phase spaces* (or equivalently *state spaces*), resulting in e.g., the  $(k, q)$  diagram (note that we dropped the adjective ‘fundamental’).

In reality, traffic is not homogeneous, nor is it stationary, thus having the effect of a large amount of scatter in the presented diagrams. In free-flow traffic, interactions between vehicles are rare, and their small local disturbances have no significant effects on the traffic stream. As a result, all points are somewhat densely concentrated along a line — representing the free-flow speed — in all four diagrams. However, in the congested regime, a wide range of scatter is visible due to the interactions between vehicles. Furthermore, vehicle accelerations and decelerations lead to large fluctuations in the traffic stream, as can be seen by the thin, but large, cloud of data points. The effect is especially pronounced for intermediate densities, leading to large fluctuations in the time-mean speed and flow.

The occurrence of all this scatter in the data, leads some traffic engineers to question the validity of the fundamental diagram. More specifically, the behaviour in congested traffic seems ill-defined to some. As stated earlier, Kerner is the most intense opponent in this debate, as he outright rejects Lighthill and Whitham’s hypothesis that remained popular over the last fifty years. Despite this criticism, the fundamental diagram remains, to the majority of the community, a fairly accurate description of the average behaviour of a traffic stream. Cassidy even provided quantifiable evidence of the existence of well-defined bivariate relations between traffic flow characteristics. The key here was to separate stationary periods from non-stationary ones in the detector data (i.e., stratifying it) [14, 27]. Prior work of Del Castillo and Benítez resulted in a more mathematically justified method, for fitting empirical curves in data regions of stationary traffic, after construction of a rigid set of properties that all fundamental diagrams should satisfy [31, 32].

As a final note, we remark that the distribution of the cloud-like data points of the diagrams in Fig. 10, is a result of various kinds of phenomena. First and foremost, there is the heterogeneity in the traffic composition (fast passenger cars, slow trailer trucks, . . .). Secondly, as already mentioned, the non-stationary behaviour of traffic introduces a significant amount of scatter in the congested regime. Thirdly, each scatter plot is dependent on the type of road, and the time of day at which the measurements were collected. In this respect, the influence of (changing) weather conditions is not to be underestimated (e.g., rain fall results in different diagrams). In conclusion, it is clear that if we want these scatter plots to better fit the fundamental diagrams, all data points should be collected under similar conditions. Even more so, the relative location on the road at which the data points were recorded plays a significant role: e.g., a jam that propagates upstream, passing an on-ramp will show different effects,

depending on where the observations were gathered (upstream, right at, or downstream of the on-ramp) and on whether or not the particular bottleneck was active [79].

### C. Capacity drop and the hysteresis phenomenon

In the early sixties, traffic engineers frequently observed a discontinuity in the measurements near the capacity flow. To this end, Edie proposed a two-regime model that included such a discontinuity at the critical density [35]. Nowadays, this typical form of the  $q_e(k)$  fundamental diagram is known as a *reversed lambda shape* (the name was originally suggested by Koshi et al. [67]).

An example of such a reversed  $\lambda$  fundamental diagram, is shown in the left part of Fig. 11. Note however, that the depicted discontinuity apparently leads to *overlapping* branches of the free-flow and congested regimes, resulting in a *multi-valued* fundamental diagram.

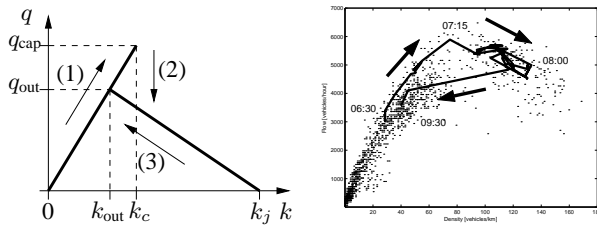


FIG. 11: *Left*: the typical inverted  $\lambda$  shape of the  $(k, q)$  fundamental diagram, showing a capacity drop from  $q_{\text{cap}}$  to below  $q_{\text{out}} \ll q_{\text{cap}}$  (i.e., the queue discharge flow). The hysteresis effect occurs when going from the congested to the free-flow branch, as indicated by the three arrows (1) – (3). *Right*: a  $(k, q)$  diagram based on empirical data of one day, obtained by video camera CLO3, at the E17 three-lane motorway near Linkeroever, Belgium. The black dots denote minute measurements, whereas the thick solid line represents the time-traced evolution of traffic conditions. The observed hysteresis loop was based on consecutive 5-minute intervals covering a period that encompasses the morning rush hour between 06:30 and 09:30.

Considering the left part of Fig. 11, it appears the flow can take on two different values (hence the name ‘two-regime, two-capacity’ model) depending on the traffic conditions, i.e., whether traffic is moving from the free-flow to the congested regime on the equilibrium curve or vice versa. In order to comprehensively understand this *hysteretic* behaviour, we consider the following intuitive sequence of events:

- (1) In the free-flow regime, the flow steadily rises with increasing density, small perturbations in the traffic flow have no significant effects (see section V A 1).
- (2) At the critical density  $k_c$ , traffic is said to be *metastable*: for small disturbances, traffic is stable, but when these disturbances are sufficiently large, they can lead to a cascading effect (see section V A 2), resulting in a breakdown of traffic and kicking it onto the congested branch. The state of capacity flow

at  $q_{\text{cap}}$  is destroyed, due to a sudden decrease of the flow, called the *capacity drop*.

- (3) In order to recover from the congested to the free-flow regime, the traffic density has to be *reduced substantially* (in comparison with the reverse transition), i.e., well below the critical density  $k_c$ . After this recovery, the flow will *not* be equal to  $q_{\text{cap}}$ , but to  $q_{\text{out}} \ll q_{\text{cap}}$ , which is called the *outflow from a jam* or the *queue discharge capacity*.

The above sequence signifies a *hysteresis loop* in the flow versus density fundamental diagram: going from the free-flow to the congested regime occurs via the capacity flow, but the reverse transition proceeds via another way. The phenomenon was first observed by Treiterer and Meyers, who used aerial photography to calculate densities and space-mean speeds, extracted from a platoon of moving vehicles [110]. Hall et al. later observed a similar phenomenon [46].

The right part of Fig. 11 shows a  $(k, q)$  diagram, obtained with empirical data collected at Monday September 10th, 2001. The data was recorded by video camera CLO3, at the E17 three-lane motorway near Linkeroever, Belgium. The small dots represent minute-based measurements, whereas the thick solid line represents the time-traced evolution of traffic conditions. The observed hysteresis loop was based on consecutive 5-minute intervals covering a period that encompasses the morning rush hour between 06:30 and 09:30.

Zhang is among the few who try to give a possible *rigorous mathematical explanation* for the occurrence of this hysteresis phenomenon [120]. His exposition is based on the behaviour of individual drivers during car-following: central to his interpretation is the existence of an *asymmetry* between accelerating and decelerating vehicles (a related notion was already explored by Newell back in 1963 [94]). The former are associated with larger space headways, whereas the latter typically have smaller space headways. Both observations can be understood when considering the characteristic ‘harmonica’ effect of a string of consecutive vehicles: when the next stop-and-go wave is encountered, a driver is more alert as he typically has to brake rather hard in order to avoid a collision. But once this wave has passed, a driver gets more relaxed, resulting in a larger response time when applying the gas pedal. The deceleration reaction leads to a sudden decrease of the space headway, whereas the acceleration reaction leads to a gradually developing larger space headway. To this end, Zhang introduces three distinct traffic phases, respectively called the *acceleration phase*, the *deceleration phase*, and a *strong equilibrium* (indicating a constant speed). Because the space headway is thus treated differently under these qualitatively different circumstances, the result is that there are now different functional relations for the  $\bar{v}_{s_e}(\bar{h}_s)$  fundamental diagram. As a consequence, a hysteresis loop can appear in the (density, flow) state space. Note that Zhang’s work describes a *continuous* loop in state space, whereas in most cases hysteresis is assumed to follow a discontinuous fundamental diagram. Furthermore, as there are three

different ways for vehicles to reside in a traffic stream (i.e., Zhang's traffic phases), there are now three different capacities related to these conditions; it is the capacity under a stationary equilibrium flow that should be considered as the ideal capacity of a roadway [121].

Note that depending on the location where the traffic stream measurements were performed, the transition from the free-flow to the congested regime and vice versa does not always have to pass via the capacity flow. Instead, observations can indicate that the traffic state can jump abruptly from one branch to another in the diagram [39]. A possible explanation is that upstream of a jam, vehicles arrive with high speeds, resulting in strong decelerations; a detector station located at this point would observe traffic jumping from the uncongested branch immediately to the congested branch, without necessarily having to pass via the capacity [95]. This has led Hall et al. to believe the reversed lambda shape is more correctly replaced by a continuous but non-differentiable *inverted V shape* [46].

Continuing this latter train of thought, Daganzo believes that many of these 'extravagant' phenomena (e.g., a multi-valued fundamental diagram) are uncalled for. Applying the stratification methodology of Cassidy [14], the scatter in the empirical data may vanish, restoring a smooth continuous equilibrium relation between density and flow. One way of explaining the high tip of the lambda, is to assume that it is caused by statistical fluctuations that comprise platoons of densely packed vehicles [27].

During the last seventy years, there has been a continuing quest to find the 'correct' form of the fundamental diagrams. In this respect, we like to stress the fact that 'only looking at the measurements' is not sufficient: traffic engineers wanting to mine the gigabytes of empirical data, should always look at the global picture. This means that the typical driving patterns, *as well as the local geometry/infrastructure*, should also be taken into account, so that the local measurements can be interpreted with respect to the traffic flow dynamics. If this is neglected, the danger exists that traffic is only sampled at discrete locations, giving a sort of 'truncated' view of the occurring dynamical processes.

Finally, we like to agree with Zhang's comments: the root cause of most of the differences in the construction of fundamental diagrams, is the erroneous treatment of data (e.g., mixing data stemming from different traffic flow regimes) [120]. Because fundamental diagrams imply the notion of an equilibrium, care should be taken when using the data, i.e., only considering stationary periods after removing the transients.

In the mid-nineties, Kerner and other fellow researchers, studied various traffic flow measurements stemming from detector stations along German motorways. Initially, they agreed with the classic notion of Lighthill and Whitham's fundamental hypothesis of the existence of one-dimensional equilibrium relation between the macroscopic traffic flow characteristics (see section V B 1 for more details). However, upon discovery of a rich and complex set of empirical tempo-spatial patterns in congested traffic flow, Kerner decided to abolish this hypothesis, as it could not adequately capture all of these observed patterns. As a consequence, Kerner rejects *all* traffic flow theories and models that are based on this one-dimensional equilibrium relation [55].

In the search for a more correct theory that could accurately describe empirical traffic flow observations, Kerner developed what is known as the *three-phase theory* of traffic flow.

#### 1. Free flow, synchronised flow, and wide-moving jam

In section V A, we elaborated on a classic approach to traffic flow, general assuming two qualitatively different regimes, namely free-flow and congested traffic. Based on empirical findings, Kerner and Rehborn in 1996 proposed three different regimes, separating the congested regime into two other regimes. This led them to the introduction of the following regimes [61]:

- free flow,
- synchronised flow,
- and wide-moving jam.

The main difference between *synchronised flow* and the *wide-moving jam*, is that in the former low speeds but high flows (comparable to free-flow traffic) can be observed, whereas in the latter both low speeds and low flows are observed. The description by the term 'synchronised' was based on the discovery that the time series of flows, densities, and mean speeds exhibited large degrees of correlation among neighbouring lanes. And although synchronised flow is treated as a form of congestion, it nevertheless is characterised by a high continuous flow. Furthermore, a typical tempo-spatial region of synchronised flow has a fixed downstream front (that could be located at a bottleneck's position), whereas both the upstream and downstream fronts of a wide-moving jam can propagate undisturbed in the upstream direction of a traffic stream [60].

Kerner distinguishes several congestion patterns with respect to traffic flows. A first typical pattern is a *synchronised-flow pattern* (SP), which can be further classified as a *moving SP* (MSP), a *widening SP* (WSP), and a *localised SP* (LSP). An SP can only contain synchronised flow; as we will shortly mention in section

VD 3, a moving jam can only occur inside such an SP. When such a jam transforms into a wide-moving jam, the resulting pattern is called a *general pattern* (GP); a GP therefore contains both synchronised flow and wide-moving jams. Just as with the SP, there exist different types of GP. These are a *dissolving GP* (DGP), a *GP under weak congestion*, and a *GP under strong congestion*. A final often encountered pattern occurs when two bottlenecks are spatially close to each other, resulting in what is called an *expanded congested pattern* (EP).

Taking the above considerations into account, the discovery and distinction between both types of congested traffic patterns should be made on the basis of tempo-spatial plots of the speed, rather than the flow (because the flow in synchronised traffic is difficult to differentiate from that of free-flow traffic) [55]. To this end, Kerner et al. developed two applications that are capable of accurately estimating, automatically tracking, and reliably predicting the above mentioned congested traffic patterns. Their models are the *Forecasting of Traffic Objects* (FOTO) and *Automatische StauDynamikAnalyse* (ASDA) [63].

## 2. Fundamental hypothesis of three-phase traffic theory

Central to Kerner's theory, is the *fundamental hypothesis of three-phase traffic theory*, which basically states that hypothetical steady states of synchronised flow, cover a *two-dimensional region* in a flow versus density diagram (as opposed to the classic notion of a one-dimensional equilibrium relation). An example of such a diagram can be seen in Fig. 12.

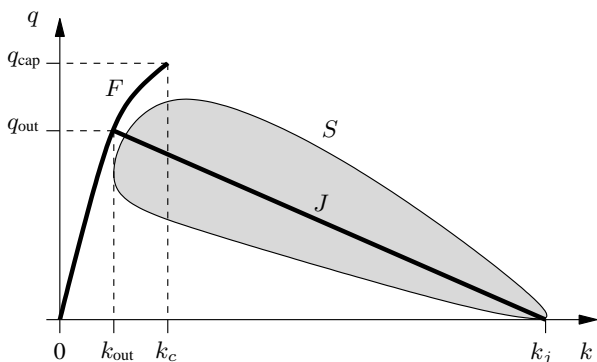


FIG. 12: The flow versus density relation according to Kerner's three-phase traffic theory. The curve of free flow (denoted by  $F$ ) is reminiscent of observations in the classic free-flow regime. It levels off a bit towards the capacity flow  $q_{\text{cap}}$  at the critical density  $k_c$ . As a result of Kerner's fundamental hypothesis, the region of synchronised flow (denoted by  $S$ ) covers a large two-dimensional part of the density-flow phase space. It is intersected by the line  $J$ , denoting the steady propagation of wide-moving jams. The line  $J$  also intersects the curve of free flow in the outflow from a jam  $q_{\text{out}} \ll q_{\text{cap}}$  at the associated density  $k_{\text{out}}$ .

In the flow versus density diagram in Fig. 12, the three regimes are depicted: the curve of free flow (denoted by  $F$ ), the region of synchronised flow (denoted by  $S$ ) and

the wide-moving jam (denoted by the empirical line  $J$ ). Just as in the classic fundamental diagrams, the observations in free-flow traffic lie on a sharp line that linearly increases the flow with higher densities (note the leveling of the curve near the capacity flow  $q_{\text{cap}}$  associated with the critical density  $k_c$ ). The region of synchronised flow spans a large part of the density-flow phase space; an important remark here is that consecutive measurement points are scattered within this region, meaning that an increase in the flow can happen with both higher *and* lower densities (as opposed to the free-flow regime) [61].

The characteristic line  $J$  denotes the steady, undisturbed propagation of wide-moving jams. Its slope corresponds to the speed of a wide-moving jam's downstream front, which typically lies around  $w \approx -15$  km/h [60]. The upper-left point of the line  $J$  is located at a density  $k_{\text{out}}$  corresponding to the outflow  $q_{\text{out}} \ll q_{\text{cap}}$  from a wide-moving jam. This is an illustration of the capacity drop phenomenon, elucidated in section VC. The line  $J$  is defined as follows:

$$q(k) = \frac{1}{T} \left( 1 - \frac{k}{k_{\text{jam}}} \right), \quad (45)$$

with  $T$  the time gap in congested traffic flows; it is used to tune the outflow from a jam. Because wide-moving jams travel undisturbed, their outflow — caused by vehicles that leave the downstream front — can be either free flow or synchronised flow. Typical values for this outflow range from 1500 to 2000 vehicles/hour/lane [55]. The average flow rate within such a wide-moving jam can be almost zero, meaning that vehicles continuously encounter stop-and-go waves.

Related to the wild scatter in the  $(k, q)$  diagram of three-phase traffic theory, is the microscopic behaviour of individual vehicles. The explanation given by Kerner and Klenov, is that vehicles in synchronised flow do not assume a fixed preferred distance to their direct frontal leader, but rather accept a certain *range of distances*. Within this range, drivers have both the tendency to over-accelerate when they think there is the ability to overtake, and the tendency for drivers to adjust their speed to that of their leader, when this overtaking can not be fulfilled [55, 58].

## 3. Transitions towards a wide-moving jam

The breakdown of traffic from the free-flow to the wide-moving jam state, is nearly always characterised by two successive  $F \rightarrow S$  and  $S \rightarrow J$  transitions, between free flow and synchronised flow, and synchronised flow and wide-moving jam respectively. In the first stage, a state of free flow changes to synchronised flow by the  $F \rightarrow S$  transition. Central to the idea of this phase transition, is the fact that there is no explicit need for an external disturbance for its occurrence. A sufficiently large (i.e., *supercritical*) internal disturbance inside the traffic stream



(e.g., a lane change) causes a *nucleation effect* that instigates the  $F \rightarrow S$  transition. Once it has set in, the onset of congestion is accompanied by a sharp drop in the mean vehicle speed. During the second stage, a set of narrow-moving jams can grow inside the tempo-spatial region of synchronised flow. A narrow-moving jam is different from a wide-moving jam, in that vehicles typically do not on average come to a full stop inside the jam. But, due to a compression of synchronised flow (an effect termed the *pinch effect*), these narrow-moving jams can coalesce into a wide-moving jam, thereby completing the cascade of the  $F \rightarrow S \rightarrow J$  transition, resulting in stop-and-go traffic [57].

With respect to the flow versus density diagram in Fig. 12, it can be seen that the line  $J$  actually divides the region of synchronised flow in two parts. Points that lie underneath this line, characterise stable traffic states where no  $S \rightarrow J$  transition can occur. Points above the line  $J$  however, characterise metastable traffic states, meaning that sufficiently large disturbances can trigger a  $S \rightarrow J$  transition [55, 66].

Note that the direct  $F \rightarrow J$  transition between free flow and wide-moving jam can also occur, but it has a very small probability, i.e., the critical perturbation needed, is much higher than that of the frequently occurring  $F \rightarrow S$  transition between free flow and synchronised flow. So in general, wide-moving jams do not emerge spontaneously in free flow, but a situation where such a transition may occur, is when an off-ramp gets filled with slow-moving vehicles. This results in a local obstruction at the motorway's lane directly adjacent to the off-ramp, which can cause a local breakdown of the upstream traffic, resulting in a wide-moving jam. Finally, it is important to distinguish the nature of this transition from that of the  $F \rightarrow S$  transition: the former is a transition *induced* by an *external disturbance* of the local traffic flow, whereas the latter is considered as a *spontaneous* transition due to an *internal disturbance* within the local traffic flow (e.g., a lane change) [55].

#### 4. From descriptions to simulations

As Kerner himself describes his three-phase theory, it is a *qualitative* theory. In essence, it gives no explanation of *why* certain transitions occur, as it only *describes* them [55]. However, several exemplary microscopic traffic flow models have already been developed (i.e., treating all vehicles and their interactions individually). These models can reproduce the different empirical tempo-spatial patterns described by Kerner's theory. As examples, we mention two models based on cellular automata: a first attempt was made by Knospe et al., who developed a model that takes into account a driver's reaction to the brake-lights of his direct frontal leader [65]. Kerner et al. refined this approach by extending it; their work resulted in a family of models based on the notion of a *synchronisation distance* for individual vehicles; they are commonly called the KKW-models (from its three authors, Kerner, Klenov, and Wolf) [56].

The theory can describe most of the encountered tempo-spatial features of congested traffic. And at the moment, successful microscopic models have been developed, but the work is not yet over: an important challenge that remains for theoreticians, is the mathematical derivation of a consistent macroscopic theory (i.e., one that treats traffic at a more aggregate level as a continuum) [55]. In pursuit of such a model, Kim incorporated Kerner's traffic regimes into a broader framework, encompassing six different possible states: the transitions between these states are tracked with a modified macroscopic model that uses concepts from fuzzy logic theory [64].

### E. Theories of traffic breakdown

A central question that is often asked in the field of traffic flow theory, is the following: "*What causes congestion ?*" Clearly, the answer to this question should be a bit more detailed than the obvious "*Because there too many vehicles on the road !*" With respect to the phase transitions that signal a breakdown of the traffic flow, various — seemingly contradicting — theories exist. Are they merely a matter of belief, or can they be rigorously 'proven' ? Opinions are divided, but nowadays, two qualitatively different mainstream theories exist, attributed to different schools of thought [12, 77, 108]:

#### The European (German) school

In the early seventies, Treiterer and Meyers performed some aerial observations of a platoon of vehicles. As they constructed individual vehicle trajectories, they could observe a growing instability in the stream of vehicles, leading to an apparently emerging *phantom jam* (i.e., a jam 'out of nothing') [110].

Some twenty years later, in the mid-nineties, Kerner and Konh user made detailed studies of traffic flow measurements, obtained at various detector stations along German motorways. Their findings indicated that phantom jams seemed to emerge in regions of unstable traffic flow [59]. This stimulated Kerner and Rehborn to further research efforts directed towards the behaviour of propagating jams [60, 61]. They proposed a different set of traffic flow regimes, culminating in what is now called *three-phase traffic theory* (see section VD for more details) [55, 57, 62]. The main idea supported by followers of this school of researchers, is that traffic jams *can* spontaneously emerge, without necessarily having an infrastructural reason (e.g., on-ramps, incidents, ...) [130]. In dense enough traffic, phase transitions from the free-flow to the synchronised-flow regime can occur, after which a local instability such as e.g., a lane change can grow (the so-called *pinch effect*), triggering a stable jam leading to stop-and-go behaviour [57]. Kerner's three-phase theory stands out as an archetypical example of these modern views. But although his theory has, in our opinion, been worked out well enough, he more than frequently encounters harsh criticisms when conveying it to most audiences (perhaps the main cause for this human behaviour is the fact that Kerner always mentions the same view, i.e., "*all existing traffic flow theories are wrong*").

Inspired by Kerner's work, Helbing et al. gave in 1999 an extended treatise on the different types of congestion patterns that can be observed in the vicinity of spatial inhomogeneities (e.g., on-ramps). Their work resulted in a universal phase diagram, containing a whole plethora of patterns of congested traffic states (called *homogeneously congested traffic* – HCT, *oscillatory congested traffic* – OCT, *triggered stop-and-go traffic* – TSG, *pinned localised cluster* – PLC, and *moving localised cluster* – MLC), each one having unique characteristics [48][131]. In that same year, Lee et al. studied the patterns that emerge at on-ramps, thereby agreeing with the findings of Helbing et al. [70]. As the previous research into congestion patterns was largely based on the use of analytical traffic flow models and computer simulations, the need for validation with empirical data grew. In 2000, the work of Treiber et al. among others, proved the existence of the previously mentioned congestion patterns [109].

At this point, it is noteworthy to mention the seminal work of Nagel and Schreckenberg [92], who in 1992 developed a model that describes traffic flows in which local jams can form spontaneously. As many variations on this model have been proposed, later work also focussed on the stability of traffic flows in these models, e.g., the work of Jost and Nagel [53].

### The Berkeley school

Including names such as the late Newell, Daganzo, Bertini, Cassidy, Muñoz, . . . , the 'Berkeley school' (University of California) supports the theory that all congestion is strictly induced by bottlenecks. The hypothesis holds for both recurrent and, in the case of an incident, non-recurrent congestion.

The main starting point states that there is *always* a 'geometrical' explanation for the breakdown. This explanation is based on the presence of road inhomogeneities such as on- and off-ramps, tunnels, weaving areas, lane drops, sharp bends, elevations, . . . Once a jam occurs due to such a (temporary) bottleneck, it does not dissipate immediately; as a result, drivers can wonder why they enter and exit a congestion wave, without there being an apparent reason for its presence (since it happened earlier and the cause e.g., an incident, already got cleared). Daganzo uses this line of reasoning as an explanation for the dismissal of phantom jams [28].

The school uses a specific terminology with respect to bottlenecks (being road inhomogeneities). Two qualitatively different regimes exist: the *free-flow regime* and the *queued regime*. The latter occurs when a bottleneck becomes *active*, which will result in a queue growing upstream of the bottleneck while a free-flow regime exists downstream. The *bottleneck capacity* is then defined as the maximum *sustainable* flow downstream (which is different from the maximum flow that can be observed prior to the bottleneck's activation).

The location of these bottlenecks has some peculiarities involved: one of them is the concept of a *capacity funnel* [11]. It assumes that drivers are at times more alert, e.g., when they are driving on a motorway and nearing an on-ramp in rather dense traffic conditions [121]. This im-

pels them to accept shorter headways, so they are driving closely behind each other at a relatively high speed. Once they have passed the on-ramp's location, they tend to relax, resulting in larger headways. The effect is that the bottleneck's *actual* position is located more downstream.

Shortly after the publication of Kerner and Rehborn's findings about the peculiar phase transitions that seemed to occur on German motorways, Daganzo et al. provided a swift response where they stated that the occurring phase transitions *could* also be caused by bottlenecks in a predictable way [29]. They implied that no spontaneously emerging traffic jams are suggested, and that the observed traffic data from both German and North American motorways did not contradict their own statements about the cause of the phase transitions [91]. In short, the subtle difference between their work and that of Kerner and Rehborn, is that instabilities in the traffic stream are the *result* and not the cause of the queues that emerge at active bottlenecks. With respect to a spontaneous breakdown of traffic flow at on- and off-ramps (i.e., bottlenecks), Daganzo also states that this can be explained using a simple traffic flow model operating under the assumption of a too high inflow from the on-ramp or a caused by blocking of the off-ramp [26].

The studies undertaken by this school, are heavily based on the researchers' use of cumulative plots and elegantly simple traffic flow models, as opposed to the classic methodology that investigates time series of recorded counts and speeds. As stated earlier (see section III B 2), some recent examples include the work of Muñoz and Daganzo [85, 86, 87, 89] and Cassidy and Bertini [7, 15].

Recently, Tampère argued that both theories, as enunciated by the two schools, are not entirely contradictory. His statement is based on the fact that the mechanisms behind the bottleneck-induced breakdown and spontaneous breakdown are approximately the same, only differing in the *probability* of such a breakdown (which is related to the instability of a traffic flow) [108].

In our view, both theories are sufficiently different, *but compatible*, in that the first school elaborately describes traffic flow breakdown more or less as having an inherently *probabilistic nature*, whereas the second school treats breakdown a strict *deterministic process*. The former introduces a complex variety of congestion patterns, while the latter primarily focusses on an elegantly simple description of traffic flow breakdown. Even more characteristically, is the observation that most adepts of the European school, *inherently need stochasticity in the models* in order to produce their sought phantom traffic jams (note that notwithstanding the fact that stochastic models are in a strict sense also deterministic, we nevertheless adopt in this dissertation, the convention that deterministic means 'non-stochastic'). Our argument is in a way also supported by Nagel and Nelson, who state that the purpose of the traffic flow model (e.g., the effect of moving bottlenecks versus predicting mean traffic behaviour) decide whether or not stochasticity in the model is required [91].

Furthermore, there might be some room for stochasticity in the Berkeley models after all, with the work of Laval which suggests that (disruptive) lane changes form the main cause for instabilities in a traffic stream [69]. Deciding which school is right, is therefore in our opinion a matter of personal taste, but in the end, we agree with Daganzo when he states that research into bottleneck behaviour is the most important in the context of traffic flow theory [30].

## VI. CONCLUSIONS

In this paper, an extensive account was given, detailing several aspects related to the description of traffic flows. Most importantly, we have introduced a nomenclature convention, built upon a consistent set of notations. Our discussion of traffic flow characteristics centred around the space and time headways as microscopic characteristics, with densities and flows as their macroscopic counterparts. Several noteworthy highlights are the technique of oblique cumulative plots and the derivation of travel times based on these plots. A finally large part of this paper reviewed some of the relations between traffic flow characteristics, i.e., the fundamental diagrams, and clarified some of the different points of view adopted by the traffic engineering community.

## APPENDIX A: GLOSSARY OF TERMS

### 1. Acronyms and abbreviations

4SM	four step model
AADT	annual average daily traffic
ABM	activity-based modelling
ACC	adaptive cruise control
ACF	average cost function
ADAS	advanced driver assistance systems
AIMSUN2	Advanced Interactive Microscopic Simulator for Urban and Non-Urban Networks
AMICI	Advanced Multi-agent Information and Control for Integrated multi-class traffic networks
AON	all-or-nothing
ASDA	Automatische StauDynamikAnalyse
ASEP	asymmetric simple exclusion process
ATIS	advanced traveller information systems
ATMS	advanced traffic management systems
BCA	Burgers cellular automaton
BJH	Benjamin, Johnso, and Hui
BJH-TCA	Benjamin-Johnson-Hui traffic cellular automaton
BL-TCA	brake-light traffic cellular automaton
BML	Biham, Middleton, and Levine
BML-TCA	Biham-Middleton-Levine traffic cellular automaton
BMW	Beckmann, McGuire, and Winsten
BPR	Bureau of Public Roads

CA	cellular automaton
CA-184	Wolfram's cellular automaton rule 184
CAD	computer aided design
CBD	central business district
CFD	computational fluid dynamics
CFL	Courant-Friedrichs-Lewy
ChSch-TCA	Chowdhury-Schadschneider traffic cellular automaton
CLO	camera Linkeroever
CML	coupled map lattice
CONTRAM	CONtinuous TRAffic Assignment Model
COMF	car-oriented mean-field theory
CPM	computational process models
CTM	cell transmission model
DDE	delayed differential equation
DFI-TCA	deterministic Fukui-Ishibashi traffic cellular automaton
DGP	dissolving general pattern
DLC	discretionary lane change
DLD	double inductive loop detector
DNL	dynamic network loading
DRIP	dynamic route information panel
DTA	dynamic traffic assignment
DTC	dynamic traffic control
DTM	dynamic traffic management
DUE	deterministic user equilibrium
DynaMIT	Dynamic network assignment for the Management of Information to Travellers
DYNASMART	DYnamic Network Assignment-Simulation Model for Advanced Roadway Telematics
ECA	elementary cellular automaton
EP	expanded congested pattern
ER-TCA	Emmerich-Rank traffic cellular automaton
FCD	floating car data
FDE	finite difference equation
FIFO	first-in, first-out
FOTO	Forecasting of Traffic Objects
GETRAM	Generic Environment for TRAffic Analysis and Modeling
GHR	Gazis-Herman-Rothery
GIS	geographical information systems
GNSS	Global Navigation Satellite System (e.g., Europe's Galileo)
GoE	Garden of Eden state
GP	general pattern
GPRS	General Packet Radio Service
GPS	Global Positioning System (e.g., USA's NAVSTAR)
GRP	generalised Riemann problem
GSM	Groupe Spéciale Mobile
GSMC	Global System for Mobile Communications
HAPP	household activity pattern problem
HCM	Highway Capacity Manual
HCT	homogeneously congested traffic
HDM	human driver model
HKM	human-kinetic model
HRB	Highway Research Board

HS-TCA	Helbing-Schreckenberg traffic cellular automaton	PLC	pinned localised cluster
ICC	intelligent cruise control	pMFT	paradisiacal mean-field theory
IDM	intelligent driver model	PRT	perception-reaction time
INDY	INteractive DYnamic traffic assignment	PSD	phase-space density
ITS	intelligent transportation systems	PW	Payne-Whitham
IVP	initial value problem	QoS	quality of service
JDK	Java™ Development Kit	SFI-TCA	stochastic Fukui-Ishibashi traffic cellular automaton
KKT	Karush-Kuhn-Tucker	Simone	Simulation model of Motorways with Next generation vehicles
KKW-TCA	Kerner-Klenov-Wolf traffic cellular automaton	SLD	single inductive loop detector
KWM	kinematic wave model	SMARTEST	Simulation Modelling Applied to Road Transport European Scheme Tests
LGA	lattice gas automaton	SMS	space-mean speed
LOD	level of detail	SOC	self-organised criticality
LOS	level of service	SOMF	site-oriented mean-field theory
LSP	localised synchronised-flow pattern	SP	synchronised-flow pattern
LTM	link transmission model	SSEP	symmetric simple exclusion process
LWR	Lighthill, Whitham, and Richards	STA	static traffic assignment
MADT	monthly average daily traffic	STCA	stochastic traffic cellular automaton
MC-STCA	multi-cell stochastic traffic cellular automaton	STCA-CC	stochastic traffic cellular automaton with cruise control
MesoTS	Mesoscopic Traffic Simulator	SUE	stochastic user equilibrium
MFT	mean-field theory	SUMO	Simulation of Urban MObility
MITRASIM	MIcrosopic TRAffic flow SIMulator	T <sup>2</sup> -TCA	Takayasu-Takayasu traffic cellular automaton
MITSIM	MIcrosopic Traffic flow SIMulator	TASEP	totally asymmetric simple exclusion process
MIXIC	Microscopic model for Simulation of Intelligent Cruise Control	TCA	traffic cellular automaton
MLC	mandatory lane change moving localised cluster	TDF	travel demand function
MOE	measure of effectiveness	TMC	Traffic Message Channel
MPA	matrix-product ansatz	TMS	time-mean speed
MPCF	marginal private cost function	TOCA	time-oriented traffic cellular automaton
MSA	method of successive averages	TRANSIMS	TRansportation ANalysis and SIMulation System
MSCF	marginal social cost function	TRB	Transportation Research Board
MSP	moving synchronised-flow pattern	TSG	triggered stop-and-go traffic
MT	movement time	UDM	ultra-discretisation method
MUC-PSD	multi-class phase-space density	UMTS	Universal Mobile Telecommunications System
NaSch	Nagel and Schreckenberg	VDR-TCA	velocity-dependent randomisation traffic cellular automaton
NAVSTAR	Navigation Satellite Timing and Ranging	VDT	total vehicle distance travelled
NCCA	number conserving cellular automaton	VHT	total vehicle hours travelled
NSE	Navier-Stokes equations	VMS	variable message sign
OCT	oscillatory congested traffic	VMT	total vehicle miles travelled
OD	origin-destination	VOT	value of time
ODE	ordinary differential equation	WSP	widening synchronised-flow pattern
OSS	Open Source Software	WYA	whole year analysis
OVF	optimal velocity function		
OVM	optimal velocity model		
Paramics	Parallel microscopic traffic simulator		
PATH	California Partners for Advanced Transit and Highways Program on Advanced Technology for the Highway		
PCE	passenger car equivalent		
PCU	passenger car unit		
PDE	partial differential equation		
PELOPS	Program for the dEvelopment of Longitudinal micrOscopic traffic Processes in a Systemrelevant environment		
PeMS	California Freeway Performance Measurement System		
PHF	peak hour factor		

## 2. List of symbols

$a_i$	the acceleration of vehicle $i$
$C$	the number of substreams in a traffic flow
$dx$	a single infinitesimal location in space
$dt$	a single infinitesimal instant in time
$\eta$	the efficiency of a road section (according to Chen et al, [18])

$E$	the efficiency of a road section (according to Brilon, [10])	$\tilde{N}(t)$	a smooth approximation of $N(t)$
$F$	the free-flow curve in three-phase traffic theory	$\bar{o}_t$	the average on-time of a set of vehicles
$g_{s_i}$	the space gap of vehicle $i$	$o_{t_i}$	the on-time of vehicle $i$
$g_{s_i}^{l,b}$	the space gap at the left-back of vehicle $i$	$o_{t_i,l}$	the on-time of vehicle $i$ in lane $l$
$g_{s_i}^{l,f}$	the space gap at the left-front of vehicle $i$	$q$	the flow
$g_{s_i}^{r,b}$	the space gap at the right-back of vehicle $i$	$\bar{q}_{ 15}$	the peak flow rate during one quarter hour within an hour
$g_{s_i}^{r,f}$	the space gap at the right-front of vehicle $i$	$\bar{q}_{ 60}$	the average flow during the hour with the maximum flow in one day
$g_{t_i}$	the time gap of vehicle $i$	$q_b$	a background flow
$g_{t_i}^{l,b}$	the time gap at the left-back of vehicle $i$	$q_c$	the flow of the $c$ -th substream in a traffic flow
$g_{t_i}^{l,f}$	the time gap at the left-front of vehicle $i$	$q_c$	the capacity flow
$g_{t_i}^{r,b}$	the time gap at the right-back of vehicle $i$	$q_{\text{cap}}$	the capacity flow
$g_{t_i}^{r,f}$	the time gap at the right-front of vehicle $i$	$q_e(k)$	an equilibrium relation between the flow and the density
$\bar{h}_s$	the average space headway	$q_l$	the flow in lane $l$
$h_{s_i}$	the space headway of vehicle $i$	$q_{\text{max}}$	the capacity flow
$h_{s_i}^{l,b}$	the space headway at the left-back of vehicle $i$	$q_{\text{out}}$	the outflow from a (wide moving) jam, the queue discharge capacity
$h_{s_i}^{l,f}$	the space headway at the left-front of vehicle $i$	$q(t)$	the flow at time $t$
$h_{s_i}^{r,b}$	the space headway at the right-back of vehicle $i$	$\rho$	the occupancy
$h_{s_i}^{r,f}$	the space headway at the right-front of vehicle $i$	$\rho_i$	the occupancy time of vehicle $i$
$\bar{h}_t$	the average time headway	$\rho_l$	the occupancy in lane $l$
$h_{t_i}$	the time headway of vehicle $i$	$R_s$	a spatial measurement region at a fixed time instant
$h_{t_i}^{l,b}$	the time headway at the left-back of vehicle $i$	$R_t$	a temporal measurement region at a fixed location
$h_{t_i}^{l,f}$	the time headway at the left-front of vehicle $i$	$R_{t,s}$	a general measurement region
$h_{t_i}^{r,b}$	the time headway at the right-back of vehicle $i$	$\sigma_s^2$	the statistical sample variance of the space- mean speed
$h_{t_i}^{r,f}$	the time headway at the right-front of vehicle $i$	$\sigma_t^2$	the statistical sample variance of the time- mean speed
$J$	the wide moving jam line $J$ in three-phase traffic theory	$S$	the synchronised-flow region in three-phase traffic theory
$k$	the density	$\tau_i$	the reaction time of vehicle $i$ 's driver
$k_c$	the density of the $c$ -th substream in a traffic flow	$t$	a time instant
$k_c$	the critical density	$T_i$	the travel time of vehicle $i$
$k_{\text{crit}}$	the critical density	$T_{\text{mp}}$	the duration of a measurement period
$k_j$	the jam density	$T(t_0)$	the experienced dynamic travel time, starting at time instant $t_0$
$k_{\text{jam}}$	the jam density	$\tilde{T}(t_0)$	the experienced instantaneous travel time, starting at time instant $t_0$
$k_{\text{max}}$	the jam density	$\bar{v}_c$	the capacity-flow speed
$k_l$	the density in lane $l$	$\bar{v}_{\text{cap}}$	the capacity-flow speed
$k_{\text{out}}$	the density associated with the queue discharge capacity	$\bar{v}_{\text{ff}}$	the free-flow speed
$k(t)$	the density at time $t$	$v_i$	the speed of vehicle $i$
$K$	the length of a measurement region (i.e., a certain road section)	$v_{i,l}$	the speed of vehicle $i$ in lane $l$
$K_{\text{ld}}$	the length of a detection zone	$v_{i,l}(t)$	the speed of vehicle $i$ in lane $l$ at time $t$
$\bar{l}$	the average length of a vehicle	$v_{\text{max}}$	the maximum allowed speed (e.g., by an imposed speed limit)
$l_i$	the length of vehicle $i$	$\bar{v}_s$	the space-mean speed
$L$	the number of lanes on a road		
$N$	the number of vehicles in a measurement region		
$N_l$	the number of vehicles in the measurement region in lane $l$		
$N_l(t)$	the number of vehicles in the measurement region in lane $l$ at time $t$		
$N(t)$	a cumulative count function		

$\bar{v}_{s_c}$	the space-mean speed of the $c$ -th substream
$\bar{v}_{s_e}(\bar{h}_s)$	an equilibrium relation between the SMS and the average space headway
$\bar{v}_{s_e}(k)$	an equilibrium relation between the SMS and the density
$\bar{v}_{s_e}(q)$	an equilibrium relation between the SMS and the flow
$\bar{v}_{\text{sust}}$	the sustained speed during a period of high flow
$\bar{v}_t$	the space-mean speed
$\bar{v}_{t_c}$	the time-mean speed of the $c$ -th substream
$v(t, x)$	the local instantaneous vehicle speed at time instant $t$ and location $x$
$w$	the characteristic/kinematic wave speed (of a wide moving jam)
$x_i$	the longitudinal position of vehicle $i$
$X_i$	the distance travelled by vehicle $i$

by: **Research Council KUL**: GOA AMBioRICS, several PhD/postdoc & fellow grants, **Flemish Government**: **FWO**: PhD/postdoc grants, projects, G.0407.02 (support vector machines), G.0197.02 (power islands), G.0141.03 (identification and cryptography), G.0491.03 (control for intensive care glycemia), G.0120.03 (QIT), G.0452.04 (new quantum algorithms), G.0499.04 (statistics), G.0211.05 (Nonlinear), research communities (IC-CoS, ANMMM, MLDM), **IWT**: PhD Grants, GBOU (McKnow), **Belgian Federal Science Policy Office**: IUAP P5/22 ('Dynamical Systems and Control: Computation, Identification and Modelling', 2002-2006), PODO-II (CP/40: TMS and Sustainability), **EU**: FP5-Quprodus, ERNSI, **Contract Research/agreements**: ISMC/IPCOS, Data4s,TML, Elia, LMS, Mastercard.

## ACKNOWLEDGEMENTS

Dr. Bart De Moor is a full professor at the Katholieke Universiteit Leuven, Belgium. Our research is supported

- 
- [1] *2000 Highway Capacity Manual*. Transportation Research Board, National Academy of Science, Washington, D.C., 2000. ISBN 9991332944.
- [2] Jorge A. Acha-Daza and Fred L. Hall. The application of catastrophe theory to traffic flow variables. *Transportation Research B*, 28B:235–250, 1994.
- [3] Luis Alvarez-Icaza, Laura Muñoz, Xiaotian Sun, and Roberto Horowitz. Adaptive observer for traffic density estimation. In *Proceedings of the 2004 American Control Conference*, pages 2705–2710, Boston, Massachusetts, June 2004.
- [4] Santiago Arroyo and Alain L. Kornhauser. Modeling travel time distributions on a road network. In *Proceedings of the 2005 TRB Annual Conference*, Washington, D.C., January 2005.
- [5] Michael Balmer, Kai Nagel, and Bryan Raney. Large-scale multi-agent simulations for transportation applications. *Journal of Intelligent Transportation Systems*, 8(4):205–222, May 2004.
- [6] Martin Beckmann, Charles Bartlett McGuire, and Christopher B. Winsten. *Studies in the Economics of Transportation*. Number RM-1488. Yale University Press, May 1955.
- [7] R.L. Bertini. Toward the systematic diagnosis of freeway bottleneck activation. In *Proceedings of the IEEE 6th Annual Conference on Intelligent Transportation Systems*, Shanghai, China, October 2003.
- [8] Robert L. Bertini, Roger V. Lindgren, Dirk Helbing, and Martin Schonhof. Empirical observations of dynamic traffic flow phenomena on a german autobahn. In *Proceedings of the 16th International Symposium on Transportation and Traffic Theory (ISTTT16)*, College Park, Maryland, July 2005.
- [9] Piet L. Bovy and Remmelt Thijs, editors. *Estimators of Travel Time for Road Networks – New developments, evaluation results, and applications*. Delft University Press, 2000. ISBN 90-407-2048-7.
- [10] Werner Brilon. Traffic flow analysis beyond traditional methods. In *Transportation Research Circular E-C018: 4th International Symposium on Highway Capacity*, pages 26–41. Transportation Research Board and National Research Council, June 2000.
- [11] D.J. Buckley and S. Yagar. Capacity funnels near on-ramps. In D.J. Buckley, editor, *Proceedings of the 6th International Symposium on Transportation and Traffic Theory*, pages 105–123, London, United Kingdom, 1974.
- [12] Stephen Budiansky. The physics of gridlock. *The Atlantic Online*, 286(6):20–24, December 2000.
- [13] M. Cassidy and J. Windover. Methodology for assessing dynamics of freeway traffic flow. *Transportation Research Record*, 1484:73–79, 1995.
- [14] Michael J. Cassidy. Bivariate relations in nearly stationary highway traffic. *Transportation Research B*, 32B(1):49–59, 1998.
- [15] M.J. Cassidy and R.L. Bertini. Some traffic features at freeway bottlenecks. *Transportation Research B*, 33B:25–42, 1999.
- [16] M.J. Cassidy and Michael Mauch. An observed traffic pattern in long freeway queues. *Transportation Research A*, 35:149–162, 2001.
- [17] R.E. Chandler, R. Herman, and E.W. Montroll. Traffic dynamics: studies in car following. *Operations Research*, 6:165–184, 1958.
- [18] Chao Chen, Zhanfeng Jia, and Pravin Varaiya. Causes and cures of highway congestion. *IEEE Control Systems Magazine*, pages 26–32, December 2001.

- [19] Chao Chen, Erik van Zwet, Pravin Varaiya, and Alex Skabardonis. *Travel Time Reliability as a Measure of Service*, 2002.
- [20] B. Coifman. Improved velocity estimation using single loop detectors. *Transportation Research A*, 35A(10):863–880, 2001.
- [21] Benjamin Coifman. Estimating density and lane inflow on a freeway segment. *Transportation Research A*, 37A(8):689–701, 2003.
- [22] Benjamin Coifman. Estimating median velocity instead of mean velocity at single loop detectors. *Transportation Research C*, 2003.
- [23] Christofer Cronström and Milan Noga. Third-order phase transition and superconductivity in thin films. *Czechoslovak Journal of Physics*, 51(2):175–184, February 2001.
- [24] Carlos F. Daganzo. The cell transmission model. part II: Network traffic. *Transportation Research B*, 29B(2):79–93, 1995.
- [25] Carlos F. Daganzo. A finite difference approximation of the kinematic wave model of traffic flow. *Transportation Research B*, 29B(4):261–276, 1995.
- [26] Carlos F. Daganzo. The nature of freeway gridlock and how to prevent it. In Jean-Baptiste Lesort, editor, *Proceedings of the 13th Symposium on Transportation and Traffic Theory*, pages 629–646, Lyon, France, July 1996.
- [27] Carlos F. Daganzo. *Fundamentals of Transportation and Traffic Operations*. Elsevier Science Ltd., 2 edition, 1997. ISBN 0-08-042785-5.
- [28] Carlos F. Daganzo. Reproducible features of congested highway traffic. *Mathematical and Computational Modeling*, (35):509–515, 2002.
- [29] Carlos F. Daganzo, Michael J. Cassidy, and Robert L. Bertini. Possible explanations of phase transitions in highway traffic. *Transportation Research A*, 33A:365–379, 1999.
- [30] C.F. Daganzo. Remarks on traffic flow modelling and its applications. *Traffic and Mobility: Simulation-Economics-Environment*, pages 105–115, July 1999. Institut für Kraftfahrwesen, RWTH Aachen, Duisburg.
- [31] J.M. Del Castillo and F.G. Benítez. On the functional form of the speed-density relationship – I: General theory. *Transportation Research B*, 29B(5):373–389, 1995.
- [32] J.M. Del Castillo and F.G. Benítez. On the functional form of the speed-density relationship – II: Empirical investigation. *Transportation Research B*, 29B(5):391–406, 1995.
- [33] C. Demir, B.S. Kerner, R.G. Herrtwich, S.L. Klenov, H. Rehborn, M. Aleksic, T. Reigber, M. Schwab, and A. Haug. FCD for urban areas: method and analysis of practical realisations. In *Proceedings of the 10th World Congress and Exhibition on Intelligent Transport Systems and Services (ITSS03)*, Madrid, Spain, November 2003.
- [34] J.S. Drake, J.L. Schofer, and A.D. May. A statistical analysis of speed density hypotheses. In L.C. Edie, R. Herman, and R. Rothery, editors, *Vehicular Traffic Science*, pages 112–117, New York, 1967. American Elsevier Publishing Company, Inc. Proceedings of the Third International Symposium on the Theory of Traffic Flow.
- [35] L.C. Edie. Car following and steady-state theory for non-congested traffic. *Operations Research*, 9:66–76, 1961.
- [36] L.C. Edie. Discussion on traffic stream measurements and definitions. In J. Almond, editor, *Proceedings of the 2nd International Symposium on the Theory of Traffic Flow*, pages 139–154, OECD, Paris, France, 1965.
- [37] B. Eisenblätter, L. Santen, A. Schadschneider, and M. Schreckenberg. Jamming transition in a cellular automaton model for traffic flow. *Physical Review E*, 57:1309–1314, 1998.
- [38] Ulrich Fastenrath. *Floating Car Data on a Larger Scale*. DDG Gesellschaft für Verkehrsdaten mbH.
- [39] Nathan Gartner, Hani Mahmassani, Carroll J. Messer, Henry Lieu, Richard Cunard, and Ajay K. Rathi. *Traffic Flow Theory: A State-of-the-Art Report*. Technical report, Transportation Research Board, December 1997.
- [40] D. Gazis, R. Herman, and R. Rothery. Nonlinear follow-the-leader models of traffic flow. *Operations Research*, 9:545–567, 1961.
- [41] D.C. Gazis, R. Herman, and R.B. Potts. Car-following theory of steady-state traffic flow. *Operations Research*, 7:499–506, 1959.
- [42] Denos C. Gazis. The origins of traffic theory. *Operations Research*, 50(1):69–77, January 2002.
- [43] H. Greenberg. An analysis of traffic flow. *Operations Research*, 7:78–85, 1959.
- [44] Bruce D. Greenshields. A study of traffic capacity. In *Highway Research Board Proceedings*, volume 14, pages 448–477, 1935.
- [45] F.A. Haight. *Mathematical theories of traffic flow*. New York Academic Press, 1963.
- [46] F.L. Hall, B.L. Allen, and M.A. Gunter. Empirical analysis of freeway flow-density relationships. *Transportation Research A*, 20A:197–210, 1986.
- [47] Dirk Helbing. *Verkehrsdynamik*. Springer-Verlag, Berlin, Heidelberg, 1997. ISBN 3-540-61927-5.
- [48] Dirk Helbing, Ansgar Hennecke, and Martin Treiber. Phase diagram of traffic states in the presence of inhomogeneities. *Physical Review Letters*, 82:4360–4363, 1999.
- [49] Dirk Helbing and Martin Treiber. Critical discussion of synchronized flow. *Cooper@tive Tr@nsport@tion Dyn@mics*, 1:2.1–2.24, 2002.
- [50] R. Herman, E.W. Montroll, R.B. Potts, and R.W. Rothery. Traffic dynamics: analysis of stability in car-following. *Operations Research*, 7:86–106, 1959.
- [51] L.H. Immers, A. Bleukx, and M. Snelder. Betrouwbaarheid van reistijden – het belang van netwerkstructuur en optimale wegcapaciteit. *Tijdschrift Vervoerswetenschappen*, 40(4):18–28, 2004.
- [52] Dominic Jost. Breakdown and recovery in traffic flow models. Master’s thesis, Department of Computer Science, ETH Zürich, August 2002.
- [53] Dominic Jost and Kai Nagel. Probabilistic traffic flow breakdown in stochastic car following models. In *Transportation Research Board Annual Meeting*, Washington, D.C., 2003. Paper 03-4266.
- [54] Christopher Kayatz. Stability analysis of traffic flow models. Master’s thesis, Eidgenössische Technische Hochschule in Zürich, August 2001.
- [55] Boris S. Kerner. *The Physics of Traffic – Empirical Freeway Pattern Features, Engineering Applications, and Theory*. Understanding Complex Systems. Springer, 2004. ISBN 3-540-20716-3.
- [56] Boris S. Kerner, Sergey K. Klenov, and Dietrich E. Wolf. Cellular automata approach to three-phase traffic theory. *Journal of Physics A: Mathematical and General*, 35:9971–10013, November 2002.
- [57] B.S. Kerner. Experimental features of self-organization in traffic flow. *Physical Review Letters*, 81(17):3797–3800, October 1998.
- [58] B.S. Kerner and S.L. Klenov. Microscopic theory of spatial-temporal congested traffic patterns at highway bottlenecks. *Physical Review E*, 68(3), September 2003.
- [59] B.S. Kerner and P. Konhäuser. Structure and parameters

- of clusters in traffic flow. *Physical Review E*, 50(1):54–83, July 1994.
- [60] B.S. Kerner and H. Rehborn. Experimental features and characteristics of traffic jams. *Physical Review E*, 53(2):1297–1300, February 1996.
- [61] B.S. Kerner and H. Rehborn. Experimental properties of complexity in traffic flow. *Physical Review E*, 53(5):4275–4278, May 1996.
- [62] B.S. Kerner and H. Rehborn. Experimental properties of phase transitions in traffic flow. *Physical Review Letters*, 79(20):4030–4033, November 1997.
- [63] B.S. Kerner, H. Rehborn, M. Aleksić, and A. Haug. Methods for tracing and forecasting of congested traffic patterns on highways. *Traffic Engineering and Control*, 42:282–287, 2001.
- [64] Youngho Kim. *Online Traffic Flow Model Applying Dynamic Flow-Density Relations*. PhD thesis, Technische Universität München, March 2002.
- [65] W. Knospé, L. Santen, A. Schadschneider, and M. Schreckenberg. Towards a realistic microscopic description of highway traffic. *Journal of Physics A: Mathematical and General*, 33:477–485, 2000.
- [66] Wolfgang Knospé. *Synchronized traffic – Microscopic modeling and empirical observations*. PhD thesis, Universität Duisburg, June 2002.
- [67] M. Koshi, M. Iwasaki, and I. Okhura. Some findings and an overview on vehicular flow characteristics. In V.F. Hurdle, E. Hauer, and G.F. Steuart, editors, *Proceedings of the 8th International Symposium on Transportation and Traffic Flow Theory*, pages 403–426, Toronto, Canada, 1983. University of Toronto Press.
- [68] S. Krauß, Kai Nagel, and Peter Wagner. The mechanism of flow breakdown in traffic flow models. In *Proceedings of the International Symposium on Traffic and Transportation Theory (ISTTT99)*, Jerusalem, 1999.
- [69] Jorge Andrés Laval. *Hybrid Models of Traffic Flow: Impacts of Bounded Vehicle Accelerations*. PhD thesis, Graduate Division of the University of California, Berkeley, 2004.
- [70] H.Y. Lee, H.-W. Lee, and D. Kim. Dynamic states of a continuum traffic equation with on-ramp. *Physical Review E*, 59(5):5101–5111, May 1999.
- [71] T.D. Lee and C.N. Yang. Statistical theory of equations of state and phase transitions: II. Lattice gas and Ising model. *Physical Review*, 87(3):410–419, August 1952.
- [72] M.J. Lighthill and G.B. Whitham. On kinematic waves: II. A theory of traffic flow on long crowded roads. In *Proceedings of the Royal Society*, volume A229, pages 317–345, 1955.
- [73] Martin Linauer and Dietrich Leihs. Generating floating car data using GSM-network. In *Proceedings of the 10th World Congress and Exhibition on Intelligent Transport Systems and Services (ITSS03)*, Madrid, Spain, November 2003.
- [74] Steven Logghe. *Dynamic modeling of heterogeneous vehicular traffic*. PhD thesis, Katholieke Universiteit Leuven, June 2003.
- [75] J.C. Luke. Mathematical models for landform evolution. *Journal of Geophysical Research*, 77:2460–2464, 1972.
- [76] Sven Maerivoet. Het gebruik van microscopische verkeerssimulatie bij een onderzoek naar de fileproblematiek op de antwerpse ring. Master’s thesis, Universitaire Instelling Antwerpen, June 2001. Promotor: prof. dr. Serge Demeyer.
- [77] Sven Maerivoet. *Traffic: an Interplay between Models, Simulations, and Control Actions*. Slides presented at the Friday Seminar (Universiteit Antwerpen), March 2004.
- [78] Sven Maerivoet and Bart De Moor. *Advancing density waves and phase transitions in a velocity dependent randomization traffic cellular automaton*. 03-111, Katholieke Universiteit Leuven, October 2004.
- [79] Adolf D. May. *Traffic Flow Fundamentals*. Prentice Hall, Englewood Cliffs, New Jersey 07632, 1990. ISBN 0-13-926072-2.
- [80] A. Messmer and M. Papageorgiou. METANET: A macroscopic simulation program for motorway networks. *Traffic Engineering and Control*, 31:466–470, 1990.
- [81] E. Michler. Statistical analysis of floating car data systems. In *8th World Congress on Intelligent Transportation Systems*, Sydney, September 2001.
- [82] E.W. Montroll and R.B. Potts. Car following and acceleration noise. In D.L. Gerlough and D.G. Capelle, editors, *An Introduction to Traffic Flow Theory*, pages 36–48, Washington, D.C., 1964. Highway Research Board. Special Report 79.
- [83] Karl Moskowitz. Waiting for a gap in a traffic stream. *Proceedings of the Highway Research Board*, 33:385–395, 1954.
- [84] Ann-Marie Mulligan and Alan Nicholson. Uncertainty in traffic flow estimation using the moving-observer method. In *IPENZ Transportation Group Conference Papers*, 2002.
- [85] Juan Carlos Muñoz and Carlos Daganzo. The bottleneck mechanism of a freeway diverge. *Transportation Research A*, 36A(6):483–505, 2000.
- [86] Juan Carlos Muñoz and Carlos Daganzo. *Experimental Characterization of Multi-lane Freeway Traffic Upstream of an Off-ramp Bottleneck*. UCB-ITS-PWP-2000-13, Partners for Advanced Transit and Highways (PATH), January 2000.
- [87] Juan Carlos Muñoz and Carlos Daganzo. Moving bottlenecks: A theory grounded on experimental observation. In M.A.P. Taylor, editor, *Proceedings of the 15th International Symposium on Transportation and Traffic Theory (ISTTT15)*, pages 441–462. Pergamon-Elsevier, 2002.
- [88] Juan Carlos Muñoz and Carlos F. Daganzo. Fingerprinting traffic from static freeway sensors. *Cooper@tive Transport@tion Dyn@mics*, 1(1):1–11, May 2002.
- [89] Juan Carlos Muñoz and Carlos F. Daganzo. Structure of the transition zone behind freeway queues. *Transportation Science*, 37(3):312–329, August 2003.
- [90] Laura Muñoz, Xiaotian Sun, Roberto Horowitz, and Luis Alvarez. Traffic density estimation with the cell transmission model. In *Proceedings of the American Control Conference*, pages 3750–3755, Denver, Colorado, June 2003.
- [91] Kai Nagel and Paul Nelson. A critical comparison of the kinematic-wave model with observational data. In Hani S Mahmassani, editor, *Proceedings of the 16th International Symposium on Transportation and Traffic Theory (ISTTT16)*. University of Maryland, July 2005.
- [92] Kai Nagel and Michael Schreckenberg. A cellular automaton model for freeway traffic. *Journal de Physique I France*, 2:2221–2229, 1992.
- [93] Kai Nagel, Peter Wagner, and Richard Woesler. Still flowing: old and new approaches for traffic flow modeling. *Operations Research*, 51(5):681–710, 2003.
- [94] Gordon F. Newell. Theories of instability in dense highway traffic. *Operations Research Society Japan*, 5:9–54, 1963.
- [95] Gordon F. Newell. *Applications of Queueing Theory*. Chapman & Hall, 2nd edition, 1982. ISBN 0412245000.
- [96] Gordon F. Newell. A simplified theory of kinematic



- waves in highway traffic, part 1: General theory. *Transportation Research B*, 27B(4):281–287, 1993.
- [97] Gordon F. Newell. A simplified theory of kinematic waves in highway traffic, part 2: Queueing at freeway bottlenecks. *Transportation Research B*, 27B(4):289–303, 1993.
- [98] Gordon F. Newell. A simplified theory of kinematic waves in highway traffic, part 3: Multi-destination flows. *Transportation Research B*, 27B(4):305–313, 1993.
- [99] Gordon F. Newell. Memoirs on highway traffic flow theory in the 1950s. *Operations Research*, 50(1):173–178, January 2002.
- [100] Phyllis Orrick. Gordon Newell memorialized at TRB. *ITS Review Online*, 1(1), July 2002.
- [101] Ilya Prigogine and Robert Herman. *Kinetic Theory of Vehicular Traffic*. Elsevier, New York, 1971.
- [102] Paul I. Richards. Shockwaves on the highway. *Operations Research*, 4:42–51, 1956.
- [103] Erik De Romph. *A Dynamic Traffic Assignment Model – Theory and Applications*. PhD thesis, Delft Technical University, Delft, The Netherlands, 1994.
- [104] Andreas Schadschneider. Traffic flow: A statistical physics point of view. *Physica A*, 313:153–187, 2002.
- [105] Terrel Shaw. *Performance Measures of Operational Effectiveness for Highway Segments and Systems*. NCHRP-Synthesis 311, National Cooperative Highway Research Program, Transportation Research Board, Washington D.C., 2003.
- [106] S.A. Smulders. *Control of Freeway Traffic Flow*. PhD thesis, University of Twente, Enschede, The Netherlands, 1989.
- [107] Henk Taale, Aad de Hoog, Stef Smulders, and Onno Tool. The results of a dutch experiment with floating car data. In *Proceedings of the 9th IFAC Symposium on Control in Transportation Systems*, volume I, Braunschweig, Germany, June 2000.
- [108] Chris M.J. Tampère. *Human-Kinetic Multiclass Traffic Flow Theory and Modelling*. TRAIL Thesis Series nr. T2004/11, TRAIL Research School, P.O. Box 5017, 2600 GA Delft, The Netherlands, December 2004.
- [109] M. Treiber, A. Hennecke, and D. Helbing. Congested traffic states in empirical observations and microscopic simulations. *Physical Review E*, 62:1805–1824, 2000.
- [110] J. Treiterer and J.A. Myers. The hysteresis phenomena in traffic flow. In D.J. Buckley, editor, *Proceedings of the 6th Symposium on Transportation and Traffic Theory*, pages 13–38, 1974.
- [111] Shawn M. Turner, William L. Eisele, Robert J. Benz, and Douglas J. Holdener. *Travel Time Data Collection Handbook*. Report FHWA-PL-98-035, Texas Transportation Institute, The Texas A&M University System, March 1998.
- [112] R.T. Underwood. Speed, volume, and density relationships – quality and theory of traffic flow. *Yale Bureau of Highway Traffic*, pages 141–188, 1961.
- [113] Verkeerscentrum Vlaanderen, Departement Leefmilieu en Infrastructuur, Administratie Wegen en Verkeer, Vuurkruisenplein 20, 2020 Antwerpen. *MINDAT – Data-bank ruwe verkeersdata Vlaams snelwegennet – 2001 en 2003*, February 2003.
- [114] Yibing Wang, Markos Papageorgiou, and Albert Messmer. Motorway traffic state estimation based on extended kalman filter. In *Proceedings of the European Control Conference ECC 03*, Cambridge, UK, September 2003.
- [115] J.G. Wardrop. Some theoretical aspects of road traffic research. In *Proceedings of the Institution of Civil Engineers*, volume 1 of 2, 1952.
- [116] J.G. Wardrop and G. Charlesworth. A method of estimating speed and flow of traffic from a moving vehicle. In *Proceedings of the Institution of Civil Engineers*, volume 3, pages 158–171, 1954.
- [117] Manfred Wermuth, Carsten Sommer, and Sven Wulff. TeleTravel Systems (TTS) – Telematic System for the Automatic Survey of Travel Behaviour. In *Proceedings of the 9th IFAC Symposium on Control in Transportation Systems*, volume I, Braunschweig, Germany, June 2000.
- [118] Marcel Westerman. *Real-Time Traffic Data Collection for Transportation Telematics*. PhD thesis, Faculty of Civil Engineering, Delft University of Technology, December 1995.
- [119] C.N. Yang and T.D. Lee. Statistical theory of equations of state and phase transitions: I. Theory of condensation. *Physical Review*, 87(3):404–409, August 1952.
- [120] H.M. Zhang. A mathematical theory of traffic hysteresis. *Transportation Research B*, 33B:1–23, 1999.
- [121] H.M. Zhang. A note on highway capacity. *Transportation Research B*, 35B:929–937, 2001.
- [122] Note that when calculating the total density using equation (5), the partial densities can also correspond without loss of generality to different vehicle classes instead of just different lanes [27, 115].
- [123] In most cases, volume denotes the number of vehicles counted during a certain time period, as opposed to flow which is just the equivalent hourly rate.
- [124] Note that the hypothesis also assumes that the variables are spatially measured, e.g., space-mean speed.
- [125] <http://www.telematicscluster.be>
- [126] Note that in a broader sense, queueing delays also encompass delays at signalled and unsignalled intersections.
- [127] The TRB was formerly known as the *Highway Research Board* (HRB).
- [128] Note that this capacity flow is not an extreme value, i.e., it can be different from the maximum observed flow. The reason is that, with respect to the nature of the fundamental diagram, the capacity flow is taken to be an *average* value [44, 72].
- [129] The detector station is called CLO3, which is an acronym for ‘Camera Linkeroever’.
- [130] But note that bottleneck-induced traffic flow breakdowns are not excluded by the theory of Kerner et al.
- [131] In addition, they also provided a link with Kerner’s three-phase theory, whereby synchronised flow can correspond to HCT, OCT, or PLC, and moving jams can correspond to TSG or MLC states [49].